ROYAL INSTITUTE
OF TECHNOLOGY

STORM in Monte Carlo reactor physics calculations

KAUR TUTTELBERG

Master of Science Thesis
Stockholm 2014

TRITA-FYS 2014:36
ISSN 0280-316X
ISRN KTH/FYS/–14:36–SE

KTH Royal Institute of Technology,
Division of Nuclear Reactor Technology,
AlbaNova University Center,
10691 Stockholm, Sweden

Tryck: Universitetsservice US AB

Abstract

This thesis was motivated primarily by the industry's needs for efficient Monte Carlo criticality solvers with advanced error estimation routines. Major effort was devoted to the study of fission source convergence, since errors present in the fission source directly affect the computed power or neutron flux distributions and other results that are collected over a number of criticality cycles. For this reason, the statistical and systematic errors in the cumulative fission source, i.e. the fission source combined over all simulated cycles, are identified in the thesis as factors determining the accuracy of the computed results. Hence, a good estimation of the errors in the cumulative fission source is crucial for correct interpretation of results from Monte Carlo criticality calculations.

This thesis presents two original methods for Monte Carlo reactor physics calculations. A novel method is suggested for estimating the error in the cumulative fission source in Monte Carlo criticality calculations by utilising the fundamental-mode eigenvector of the fission matrix. While statistical errors are present in the eigenvector, it appears that these are only weakly correlated to the errors in the cumulative fission source. This ensures that the suggested method gives error estimates that are distributed around the real errors, which is also supported by results of numerical test calculations. This method has been described in a journal manuscript that was accepted for publication in Annals of Nuclear Energy.

Another, related, method is suggested for improving the efficiency of Monte Carlo reactor physics criticality calculations. This is achieved by optimising the number of neutron histories simulated per criticality cycle (the so-called neutron batch size). This is possible as the chosen neutron batch size affects both the rate of convergence and magnitude of bias in the fission source. For instance, setting a small neutron batch size ensures a rapid simulation of criticality cycles, allowing the fission source to converge fast to its stationary state; however, at the same time, the small neutron batch size introduces a relatively large systematic bias in the fission source. Hence, for a given allocated computing time, there is an optimal neutron batch size that balances these two effects. This optimisation problem is approached by deriving a simplified formula for the scalar error in the cumulative fission source, taking into account the neutron batch size, the dominance ratio of the system, the error in the initial fission source and the total number of neutron histories to be simulated. Knowledge of how the neutron batch size affects the error in the cumulative fission source allows its optimal value to be found. This is demonstrated on a number of numerical test calculations. This method has been described in another journal manuscript that was submitted for publication to Annals of Nuclear Energy.

The suggested methodologies allow for more efficient Monte Carlo reactor physics calculations, giving results with errors that can be estimated more reliably than with other existing methods. The suggested methods can easily be implemented in established Monte Carlo criticality codes.

Included papers

1. Tuttelberg, K., Dufek, J. Estimation of errors in the cumulative Monte Carlo fission source. *Annals of Nuclear Energy.* Accepted for publication, 2014.

2. Tuttelberg, K., Dufek, J. Neutron batch size optimisation methodology for Monte Carlo criticality calculations. *Annals of Nuclear Energy.* Submitted for publication, 2014.

Contents

Preface

The work that became this thesis is the result of a close collaboration between me and Jan Dufek, whose research it was meant to support. The presented research was carried out at the Nuclear Reactor Technology division of KTH Royal Institute of Technology.

First and foremost I would like to thank my supervisor, Jan Dufek for providing me with an interesting and challenging topic to work on, and for encouraging me to write the papers that constitute the thesis. I would also like to thank Vasily Arzhanov for helping me in tackling various mathematical challenges. Lastly, I would like to give my regards to all the people who made this year at KTH as pleasant and memorable as it was.

This research was supported by Estonian scholarship program Kristjan Jaak, which is funded and managed by Archimedes Foundation in collaboration with the Ministry of Education and Research.

"There are times I find mathematics totally awesome. It just blows me away. It's not the math itself and it's not the physical reality itself that I find awesome, but it's the link between the mathematics and physical reality. The fact that mathematics actually successfully models reality, it just blows me away, you know."

Prof. William J. Garland

Chapter 1

Introduction

1.1 Neutron transport problems

Neutron transport, or neutronics, is a branch of reactor physics and nuclear engineering that studies how neutrons behave in a system; where behaviour means the distribution and physical properties of neutrons. The study of neutron transport is employed in various nuclear engineering applications. [37]

The distribution and properties of neutrons are commonly described by phase-space density (or alternatively, angular flux), which is a mathematical quantity specifying the number of neutrons at any point in time and space, with a certain energy and movement direction. This is the fundamental quantity in the neutron transport equation and its simplified variant, the neutron diffusion equation—the mathematical models of neutron transport. [7]

In reactor physics, neutron transport is studied because the phase-space density (or flux) is related to the power of the reactor, criticality of the system, and other phenomena. [7] It is also relevant in other areas of nuclear engineering, like fuel and waste storage, radiation shielding, and other applications. Transport calculations may also be coupled to thermal hydraulic and fuel burn-up solvers.

Nuclear power plants, like many other types of power generating units, require tools for design, analysis, and fuel planning. Neutron transport (and especially criticality) calculations play an important part in both reactor design and analysis and fuel cycle management, making it important to further develop the necessary tools. The work presented in this thesis concentrates on and attempts to further improve one of these tools—the Monte Carlo criticality method.

1.2 Characteristics of Monte Carlo criticality calculations

Most methods of solving the neutron transport equation make significant simplifications due to the sheer complexity of the mathematical model. The approach of

statistical sampling employed in Monte Carlo calculations allows the quantities of interest to be estimated without actually solving the transport equation. Individual neutrons are simulated by sampling events from known probability distributions and the expected behaviour is found as an average. [4] Different physical phenomena can be described more realistically and the least number of simplifications is needed, making the Monte Carlo method potentially the most accurate approach. However, due to its simulative nature, it is also the most computationally demanding method.

The different physical phenomena and the geometry may be described in a very detailed manner, but with today's computers the number of simulated particles cannot come close to the actual number of neutrons in the system. If a real system may have, to the order of magnitude, 10^{15} or 10^{18} neutrons per unit volume in unit time, then a longer Monte Carlo calculation may simulate some millions of neutrons in the whole system per iteration cycle. A large number of cycles has to be simulated to obtain good estimates for the averaged values. What is more, in criticality calculations the fission source, where the neutrons are sampled from, is also not known and has to be estimated iteratively during the calculation. If the fission source itself is not estimated correctly enough, all other quantities become erroneous.

The precision of Monte Carlo calculations is determined by the total number of simulated neutrons and commonly described by variances of estimated quantities. The time spent on the calculation is also largely proportional to the total number of simulated particles, which is determined by the product of iterated cycles and number of neutrons simulated per cycle (the neutron batch size). The ratio of these two values, however, has two different implications on the accuracy of results. Firstly, a large number of cycles may be needed to converge the fission source from the initial guess to an accurate distribution. Secondly, simulating a small number of neutrons per cycle introduces systematic errors in the fission source. These are systematic problems affecting accuracy and neither of them is reflected in the calculated variance estimates. [13]

1.3 Objective and structure of thesis

The first aim of this thesis is to specify a quantity that captures real calculation errors introduced by different phenomena and find ways to estimate these errors. All obtained results of Monte Carlo criticality calculations are combined over a number of cycles, and are directly affected by the errors in the fission source. Thus, the error in the cumulative fission source (the fission source combined over all simulated cycles) is chosen to represent the error of the calculation. The second goal is to find a simplified model for these errors and utilise it to optimise the calculations for increased efficiency. The figure of merit is related to the modelled error and available computational time and maximised by optimising the neutron batch size.

The author of the thesis has prepared two publications, the first of which presents a new error estimation method and the second proposes a way to improve the efficiency of calculations by optimising the neutron batch size. The concepts introduced in these papers are presented as the main part of the thesis.

Chapter 2 provides a background overview of the topic; it introduces the neutron transport equation and its eigenvalue variant, summarises the basics of statistical sampling, and describes the concepts of Monte Carlo criticality methods. This is followed by a mathematical description of Monte Carlo eigenvalue calculations in Chapter 3, where different aspects of fission source convergence and errors of calculations are analysed. Chapter 4 proposes a way to estimate errors in the cumulative Monte Carlo fission source, based on the eigenvector of the fission matrix. In Chapter 5, a simplified model is derived for the error in the cumulative source and used to derive an optimal value for the neutron batch size; additionally, a methodology is offered for implementation of the optimisation. The work is summarised in Chapter 6.

Chapter 2

Monte Carlo methods in reactor physics

"One Does not simply solve the neutron transport equation."

The Boromir one-does-not-simply meme

2.1 Neutron transport equation

The aim of neutron transport theory is to describe how neutrons move in space and interact with materials. It attempts to determine where neutrons are, what velocity they have and which direction they are moving in. The quantity that captures all of that information is called neutron phase-space density and denoted as $N(\mathbf{r}, \mathbf{v}, t)$, so that

$$N(\mathbf{r}, \mathbf{v}, t)\mathrm{d}\mathbf{r}\mathrm{d}\mathbf{v}$$

is the expected number of particles located at $\mathbf{r}$ in volume $\mathrm{d}\mathbf{r}$ moving with a velocity in a direction specified by $\mathbf{v}$ in $\mathrm{d}\mathbf{v}$ at time t. [7] Both $\mathbf{r}$ and $\mathbf{v}$ are three-dimensional vectors, one specifying position and the other direction and speed.

This is a basic quantity containing the necessary information to analyse a nuclear system. By knowing neutron phase-space density, one can determine the power distribution in a nuclear reactor, calculate various reaction rates or evaluate some other quantity of interest.

Neutron density $n(\mathbf{r}, t)$ in the system can be found as an integral quantity of the phase-space density by integrating over velocity

$$n(\mathbf{r}, t) = \int N(\mathbf{r}, \mathbf{v}, t)\mathrm{d}\mathbf{v} \tag{2.1}$$

When describing neutron transport, the velocity vector is often decomposed into a vector describing direction and a scalar term for velocity, or speed. The speed is

taken as $v = |\mathbf{v}|$ and the direction term is described as $\mathbf{\Omega} = \mathbf{v}/v$. Often, instead of using speed as a variable, it is replaced by the kinetic energy $E = mv^2/2$. [7]

Now the following can be written

$$N(\mathbf{r}, \mathbf{\Omega}, E, t)\mathrm{d}\mathbf{r}\mathrm{d}\mathbf{\Omega}\mathrm{d}E$$

as the number of neutrons at $\mathbf{r}$ in volume $\mathrm{d}\mathbf{r}$ moving in the direction $\mathbf{\Omega}$ in solid angle $\mathrm{d}\mathbf{\Omega}$ with energy E in $\mathrm{d}E$ at time t.

Having these initial formalisms laid out, the formation of the neutron transport equation can be started. As a balance equation, it simply considers the gains and losses of particles. This balance can be understood so that the sum of changes due to leakage, collisions, and sources is equal to the time rate of change in phase-space particle density.

The equation can be derived in the simplest manner by assuming that the substantial derivative of phase-space density along the particle trajectory is equal to changes due to collisions and sources. [7] This is expressed as

$$\frac{\mathrm{d}N(\mathbf{r}, \mathbf{v}, t)}{\mathrm{d}t} = \left(\frac{\partial N}{\partial t}\right)_{coll} + q(\mathbf{r}, \mathbf{v}, t) \tag{2.2}$$

where q is the source term. Following that, it can be shown that

$$\frac{\mathrm{d}N}{\mathrm{d}t} = \frac{\partial N}{\partial t} + \mathbf{v}\frac{\partial N}{\partial \mathbf{r}} + \frac{\mathbf{F}}{m} \cdot \frac{\partial N}{\partial \mathbf{v}} \tag{2.3}$$

The last term in this equation describes effects caused by gravity, which can be considered negligible and disregarded in neutron transport. [7]

Considering this result and denoting $\partial N/\partial \mathbf{r} = \nabla N$, the time rate of change in phase-space density N becomes

$$\frac{\partial N(\mathbf{r}, \mathbf{v}, t)}{\partial t} = -\mathbf{v}\nabla N(\mathbf{r}, \mathbf{v}, t) + \left(\frac{\partial N}{\partial t}\right)_{coll} + q(\mathbf{r}, \mathbf{v}, t) \tag{2.4}$$

which is a mathematical representation of the previously stated balance of gains and losses. This is a general form of the neutron transport equation. [7]

In order to describe the changes due to collisions, some additional definitions are called for. The collisions or interactions with the surrounding medium are assumed to happen instantaneously at some point in space. Particles are assumed to be streaming along until a point of collision, after which they are either absorbed or scattered in a new direction at a new velocity.

Firstly, the probability for a particle to have an interaction at a location $\mathbf{r}$ per unit distance travelled at velocity $\mathbf{v}$ is defined as the macroscopic cross section $\Sigma(\mathbf{r}, \mathbf{v})$. It is also described as the inverse of the mean free path *mfp* and related to the

microscopic cross section[1] σ by the number density N_B of the surrounding medium as

$$\Sigma(\mathbf{r}, \mathbf{v}) = N_B(\mathbf{r})\sigma(\mathbf{v}) = mfp^{-1} \tag{2.5}$$

Transport theory is used to describe how particles moving through a medium undergo collisions and scatterings. In order to describe these interaction processes, where the incident particle is absorbed and secondary particles are emitted, a scattering probability function $f(\mathbf{r}, \mathbf{v}' \to \mathbf{v})$ is defined, so that

$$f(\mathbf{r}, \mathbf{v}' \to \mathbf{v})\mathrm{d}\mathbf{v}$$

gives the probability that an incident particle travelling at velocity $\mathbf{v}'$ causes the emission of any particles at $\mathbf{r}$ with velocity $\mathbf{v}$ in $\mathrm{d}\mathbf{v}$.

Following that, the quantity $c(\mathbf{r}, \mathbf{v})$ is defined as the mean number of secondary particles emitted after an incident particle collides at $\mathbf{r}$, travelling at $\mathbf{v}$. The previous three definitions can then be combined into a collision kernel, which is defined as

$$\Sigma(\mathbf{r}, \mathbf{v}' \to \mathbf{v}) = \Sigma(\mathbf{r}, \mathbf{v})c(\mathbf{r}, \mathbf{v})f(\mathbf{r}, \mathbf{v}' \to \mathbf{v}) \tag{2.6}$$

This kernel can be viewed as the probability that an incident particle travelling at $\mathbf{v}'$ will have a collision per unit distance which results in the emission of a particle with velocity $\mathbf{v}$. Now, by definition

$$\Sigma(\mathbf{r}, \mathbf{v}) = \int \Sigma(\mathbf{r}, \mathbf{v}' \to \mathbf{v})\mathrm{d}\mathbf{v}' \tag{2.7}$$

Next it can be noted that the products

$$v\Sigma(\mathbf{r}, \mathbf{v})$$
$$v\Sigma(\mathbf{r}, \mathbf{v})N(\mathbf{r}, \mathbf{v}, t)$$

describe collision frequency and reaction rate density, respectively. It can be reasoned that the loss rate by collisions for particles with velocity $\mathbf{v}$ is then described by $v\Sigma(\mathbf{r}, \mathbf{v})N(\mathbf{r}, \mathbf{v}, t)$ and the production of secondary particles travelling at $\mathbf{v}$ caused by particles with velocities $\mathbf{v}'$ is given by $v'\Sigma(\mathbf{r}, \mathbf{v}' \to \mathbf{v})N(\mathbf{r}, \mathbf{v}', t)\mathrm{d}\mathbf{v}'$. This results in the following expression for the collision term

$$\left(\frac{\partial N}{\partial t}\right)_{coll} = \int v'\Sigma(\mathbf{r}, \mathbf{v}' \to \mathbf{v})N(\mathbf{r}, \mathbf{v}', t)\mathrm{d}\mathbf{v}' - v\Sigma(\mathbf{r}, \mathbf{v})N(\mathbf{r}, \mathbf{v}, t) \tag{2.8}$$

so that the general form of the transport equation becomes [7]

$$\frac{\partial N}{\partial t} + \mathbf{v}\nabla N + v\Sigma N = \int v'\Sigma(\mathbf{r}, \mathbf{v}' \to \mathbf{v})N(\mathbf{r}, \mathbf{v}', t)\mathrm{d}\mathbf{v}' + q \tag{2.9}$$

[1] The microscopic cross section is a quantity describing probabilities of interaction events as effective collision areas

where $N = N(\mathbf{r}, \mathbf{v}, t)$ and $q = q(\mathbf{r}, \mathbf{v}, t)$.

Due to the frequent use of the product vN in reaction rates, it is common to define the angular, or phase-space, neutron flux as

$$\Phi(\mathbf{r}, \mathbf{v}, t) = vN(\mathbf{r}, \mathbf{v}, t) \tag{2.10}$$

and the velocity integrated, or scalar, flux as

$$\phi(\mathbf{r}, t) = \int \Phi(\mathbf{r}, \mathbf{v}, t)\mathrm{d}\mathbf{v} = \int vN(\mathbf{r}, \mathbf{v}, t)\mathrm{d}\mathbf{v} \tag{2.11}$$

The transport equation can then be written in terms of angular flux

$$\frac{1}{v}\frac{\partial \Phi}{\partial t} + \mathbf{\Omega}\nabla\Phi + \Sigma\Phi = \int_{4\pi}\int_{0}^{\infty} \Sigma(\mathbf{r}, \mathbf{\Omega}', E' \to \mathbf{\Omega}, E)\Phi(\mathbf{r}, \mathbf{\Omega}', E', t)\mathrm{d}\mathbf{\Omega}'\mathrm{d}E' + q \tag{2.12}$$

It is common to separate the collision kernel into two components, one describing fission events and the other scatterings. This is done so that

$$\Sigma(\mathbf{r}, \mathbf{\Omega}', E' \to \mathbf{\Omega}, E) = \Sigma_f(\mathbf{r}, \mathbf{\Omega}', E' \to \mathbf{\Omega}, E) + \Sigma_{sc}(\mathbf{r}, \mathbf{\Omega}', E' \to \mathbf{\Omega}, E) \tag{2.13}$$

where the index f denotes fission and sc scattering.

In general it is considered that as a good assumption fission neutrons can be treated as being emitted isotropically in the laboratory reference system. Having this in mind, the related scattering probability is described as

$$f_f(\mathbf{r}, \mathbf{\Omega}', E' \to \mathbf{\Omega}, E)\mathrm{d}\mathbf{\Omega}\mathrm{d}E = \frac{1}{4\pi}\nu(\mathbf{r}, E' \to E)\mathrm{d}\mathbf{\Omega}\mathrm{d}E \tag{2.14}$$

where $\nu(\mathbf{r}, E' \to E)$ is referred to as the fission neutron energy spectrum, i.e. the probability that a fission induced by a neutron at $\mathbf{r}$ with energy E' will produce a neutron with energy E in $\mathrm{d}E$. This spectrum is further separated into two components as

$$\nu(\mathbf{r}, E' \to E) = \chi(\mathbf{r}, E' \to E)\nu(\mathbf{r}, E') \tag{2.15}$$

where $\nu(\mathbf{r}, E') = \int \nu(\mathbf{r}, E' \to E)\mathrm{d}E$ is the average number of neutrons produced by a fission caused by a neutron with energy E' at $\mathbf{r}$. The term $\chi(\mathbf{r}, E' \to E)$ is the normalized fission spectrum. It has been established that the dependence of χ on incident energy can be ignored. This means $\chi(\mathbf{r}, E' \to E) = \chi(\mathbf{r}, E)$, which can be considered as the distribution of energies for produced fission neutrons. [7]

Based on this, the fission term in the collision kernel becomes

$$\Sigma_f(\mathbf{r}, \mathbf{\Omega}', E' \to \mathbf{\Omega}, E) = \frac{\chi(\mathbf{r}, E)}{4\pi}\nu(\mathbf{r}, E')\Sigma_f(\mathbf{r}, E') \tag{2.16}$$

This enables the transport equation to be written as

$$\frac{1}{v}\frac{\partial\Phi}{\partial t}+\mathbf{\Omega}\nabla\Phi+\Sigma\Phi=\int_{4\pi}\int_{0}^{\infty}\Sigma_{sc}(\mathbf{r},\mathbf{\Omega}',E'\rightarrow\mathbf{\Omega},E)\Phi(\mathbf{r},\mathbf{\Omega}',E',t)\mathrm{d}\mathbf{\Omega}'\mathrm{d}E'+$$
$$+\frac{\chi(\mathbf{r},E)}{4\pi}\int_{4\pi}\int_{0}^{\infty}\nu(\mathbf{r},E')\Sigma_{f}(\mathbf{r},E')\Phi(\mathbf{r},\mathbf{\Omega}',E',t)\mathrm{d}\mathbf{\Omega}'\mathrm{d}E'+q \tag{2.17}$$

which is then complemented by appropriate initial and boundary conditions.

In a case when the equation does not contain a source term, i.e. $q=0$, the equation is considered to be homogeneous and linear. The linearity here means that any linear combination of some arbitrary solutions Φ_1 and Φ_2 of the transport equation is also a valid solution. [7]

2.1.1 *k*-eigenvalue equation

The criticality of nuclear systems is studied with eigenvalue equations. Firstly, a system is considered sub-critical if the fission reactions cannot sustain a neutron population without an extraneous source and the population disappears over time. If the neutron population keeps growing over time, the system is supercritical, and if it remains steady with no source present, it can be considered critical.

One major type of eigenvalue equations is formed by introducing auxiliary eigenvalues into the steady state homogeneous transport equation. This is commonly done by modifying the term $\nu(\mathbf{r},E')$ so that it reads $\nu(\mathbf{r},E')/k$. In effect, this means that the number of produced fission neutrons is divided by a factor, commonly known as the effective multiplication factor k_{eff}. The steady state ($\partial\Phi/\partial t=0$) k-eigenvalue equation can then be written as

$$\mathbf{\Omega}\nabla\Phi+\Sigma\Phi=\int_{4\pi}\int_{0}^{\infty}\Sigma'_{sc}\Phi'\mathrm{d}\mathbf{\Omega}'\mathrm{d}E'+\frac{1}{k}\int_{4\pi}\int_{0}^{\infty}\frac{\chi}{4\pi}\nu\Sigma'_{f}\Phi'\mathrm{d}\mathbf{\Omega}'\mathrm{d}E' \tag{2.18}$$

where the quantities with primes are $\Phi'=\Phi(\mathbf{r},\mathbf{\Omega}',E')$, $\Sigma'_{sc}=\Sigma_{sc}(\mathbf{r},\mathbf{\Omega}',E'\rightarrow\mathbf{\Omega},E)$ and $\nu\Sigma'_{f}=\nu(\mathbf{r},E')\Sigma_{f}(\mathbf{r},E')$. [7]

The terms in this equation can be combined into two operators. Firstly, the transport operator is formed as [33]

$$T\Phi(\mathbf{r},\mathbf{\Omega},E)=\mathbf{\Omega}\nabla\Phi+\Sigma\Phi-\int_{4\pi}\int_{0}^{\infty}\Sigma'_{sc}\Phi'\mathrm{d}\mathbf{\Omega}'\mathrm{d}E' \tag{2.19}$$

and secondly, the fission source as [3]

$$s(\mathbf{r})=\int_{4\pi}\int_{0}^{\infty}\nu\Sigma'_{f}\Phi'\mathrm{d}\mathbf{\Omega}'\mathrm{d}E' \tag{2.20}$$

Using these two operators, the k-eigenvalue equation can be written as

$$k_j T\Phi_j(\mathbf{r}, \mathbf{\Omega}, E) = \frac{\chi(E)}{4\pi} s_j(\mathbf{r}) \tag{2.21}$$

where k_j are the eigenvalues and Φ_j (with the corresponding s_j) the eigenfunctions of the steady-state transport equation and $\chi(E)$ is the energy spectrum of emitted fission neutrons. As a simplification, $\chi(E)$ is assumed to be independent of the energy of the neutrons causing fission; and fission neutron emission is assumed to be isotropic. [3]

The eigenvalue spectrum is commonly ordered descendingly, starting with the highest modulus eigenvalue being denoted by k_0, so that

$$k_0 > |k_1| > |k_2| > \dots$$

The highest modulus eigenvalue corresponds to the fundamental mode eigenfunction Φ_0 and is equated with the effective multiplication factor, i.e. $k_{\text{eff}} = k_0$. Considering the nature of eigenfunctions, only the fundamental mode solution is positive throughout the system, which means that only Φ_0 is related to a physically meaningful angular neutron flux. [7]

The k-eigenvalue is related to criticality so that $k_{\text{eff}} = 1$ implies that the system is critical, $k_{\text{eff}} < 1$ shows sub-criticality, and $k_{\text{eff}} > 1$ means the system is supercritical.

2.1.2 Solving the transport equation

The neutron transport equation is essentially an exact description of transport processes as long as the cross sections are described sufficiently well. The solution for neutron phase space density or angular neutron flux would provide all the information that could be required. However, in the general case, this equation does not have an analytic solution.

The transport equation contains seven independent variables: position (x, y, z in $\mathbf{r}$), direction (θ, φ in $\mathbf{\Omega}$), energy (E), and time (t). In addition to that, the cross sections are dependent on materials and particle energies. All of this combined with the nature of this integro-differential equation makes it very difficult to solve. [7]

Possible approaches to solving the equation could be divided into three categories. The first way would be to simplify the transport equation itself to an extent allowing it to be applied to realistic problems. This group includes approximations like diffusion theory or P_N equations. The second type of approach would be to only consider problems that are possible to be analysed analytically. This group contains problems with either very simple geometry or strong simplifications in energy or angular dependence. The third approach would be to solve the transport equation numerically, either by deterministic or stochastic methods. This group enables higher complexity in both the mathematical representation of the transport equation and the system being studied. [7]

The last of these groups includes solving the equation by stochastic or statistical sampling, also known as the Monte Carlo method. The fundamentals of the Monte Carlo method and its application to criticality problems are presented in the next sections.

2.2 Basics of statistical sampling

2.2.1 Stochastic quantities

A random variable X is a variable that obtains a value x (a realisation) by random selection from a set of possible values. A discrete random variable may obtain a value x_i from a finite set of values $\{x_1, x_2, \ldots, x_n\}$ with a probability $p_i = P(X = x_i)$. A continuous random variable may obtain a value x from an infinite set of values with probabilities described by a probability distribution function. [20] The cumulative distribution function (cdf) is defined as the probability of a continuous random variable X obtaining a value that is smaller than or equal to x

$$F_X(x) = P(X \leq x) = \int_{-\infty}^{x} f_X(\xi)\mathrm{d}\xi \tag{2.22}$$

The probability density function (pdf) is expressed as

$$f_X(x) = \frac{\mathrm{d}F_X(x)}{\mathrm{d}x} \tag{2.23}$$

and is characterised by the following identity

$$\int_{-\infty}^{\infty} f_X(x)\mathrm{d}x = 1 \tag{2.24}$$

For discrete random variables an analogous identity is given as

$$\sum_{i=1}^{n} p_i = 1 \tag{2.25}$$

The expected value of a continuous random variable X is defined as

$$\mathrm{E}[X] = \int_{-\infty}^{\infty} x f_X(x)\mathrm{d}x \tag{2.26}$$

whereas the equivalent quantity for a discrete random variable X is [20]

$$\mathrm{E}[X] = \sum_{i=1}^{n} p_i x_i \tag{2.27}$$

which is an average of all possible values weighted by their probabilities.

To measure how spread out a set of values is, a quantity known as variance is used. The variance of a random variable X is defined as

$$\mathrm{Var}\left[X\right] = \mathrm{E}\left[\left(X - \mathrm{E}\left[X\right]\right)^2\right] = \mathrm{E}\left[X^2\right] - \left(\mathrm{E}\left[X\right]\right)^2 \tag{2.28}$$

where the last equality can be verified by properties of the expected value. [20] Following that, the standard deviation is defined as

$$\sigma_X = \sqrt{\mathrm{Var}\left[X\right]} \tag{2.29}$$

which characterises the dispersion of realisations from the expected value.

To analyse how two different random variables, say X and Y, are related, the covariance is defined as

$$\mathrm{Cov}\left[X, Y\right] = \mathrm{E}\left[\left(X - \mathrm{E}\left[X\right]\right)\left(Y - \mathrm{E}\left[Y\right]\right)\right] = \mathrm{E}\left[XY\right] - \mathrm{E}\left[X\right]\mathrm{E}\left[Y\right] \tag{2.30}$$

Based on this, another measure, the correlation coefficient is defined as

$$\rho_{XY} = \frac{\mathrm{Cov}\left[X, Y\right]}{\sigma_X \sigma_Y} \tag{2.31}$$

which is a coefficient in the range $[-1, 1]$. Correlation is used to measure dependence between two random variables. However, it has to be noted that dependence implies correlation but correlation does not always mean dependence.

2.2.2 Sampling methods

A Monte Carlo procedure can be viewed in a simple manner by assuming an unknown random variable Y that is estimated by a mathematical model g using samples of an input random variable X, so that [8]

$$Y = g(X) \tag{2.32}$$

Here the distribution function is known for X but unknown for Y, and the model g is complicated enough to prevent the direct calculation of the expected value of Y. In order to estimate Y, some n values are sampled for X and corresponding values of $g(X)$ are calculated. This produces n samples for Y as $y_i = g(x_i)$.

Sampling is the act of drawing a random variable from a distribution function describing some phenomenon. There is a large variety of sampling methods and algorithms to achieve this, the description of which is not in the scope of this work. Sampling relies on random number generators (RNG) for which there is also a wide range of algorithms. The purpose of an RNG is to provide random (or seemingly random) values from a certain probability distribution. [20]

The expected value of the random variable Y is then estimated based on the sampled values by taking their mean, or ensemble average, value

$$\bar{y} = \langle y_n \rangle = \frac{1}{n} \sum_{i=1}^{n} y_i \tag{2.33}$$

and the assumption $\mathrm{E}[Y] \cong \bar{y}$.

The variance of the mean is commonly estimated by the sample variance

$$\mathrm{Var}\,[\,\bar{y}\,] \cong \sigma_S^2 = \frac{1}{n(n-1)} \sum_{i=1}^{n} (y_i - \bar{y})^2 = \frac{1}{n-1} \left(\overline{y^2} - \bar{y}^2 \right) \tag{2.34}$$

which is a good estimate if the samples are not correlated or the correlation is weak. [22] However, since this assumption is not always correct, it is important to note that this estimate does not always capture the real error, even if the number of samples is increased. [13] The real variance would be, according to the definition

$$\sigma_R^2 = \mathrm{E}\left[Y^2\right] - \left(\mathrm{E}\,[Y]\right)^2 \tag{2.35}$$

Different ways have been suggested [17, 22, 31, 33, 36] to evaluate the so-called variance bias $\sigma_S^2 - \sigma_R^2$, but the problem is nevertheless present.

Commonly, the efficiency of a Monte Carlo calculation is described by the figure of merit, defined as

$$\mathrm{FOM} = \frac{1}{\sigma^2 t} \tag{2.36}$$

where t is the computational time spent on the calculation and $\sigma^2 \cong \sigma_S^2$ is the estimated variance of the quantity of interest.

2.3 Monte Carlo criticality calculations

The idea of using statistical sampling to solve neutron transport problems was introduced in the correspondence of J. von Neumann and R. D. Richtmyer as

> "... a method of solving neutron diffusion problems in which data are chosen at random to represent a number of neutrons in a chain-reacting system. The history of these neutrons and their progeny is determined by detailed calculations of the motions and collisions of these neutrons, randomly chosen variables being introduced at certain points in such a way as to represent the occurrence of various processes with the correct probabilities. If the history is followed far enough, the chain reaction thus represented may be regarded as a representative sample of a chain reaction in the system in question. The result may be analyzed statistically to obtain various average quantities of interest for comparison with

> experiments or for design problems. [—] It is not necessary to restrict neutron energies to a single value or even to a finite number of values and one can study the distribution of neutrons or of collisions of any specified type not only with respect to space variables but with respect to other variables, such as neutron velocity, direction of motion, time." [28]

The Monte Carlo method solves neutron transport problems by simulating individual particles and recording aspects of their behaviour. The average behaviour of particles in the system is then found based on the average behaviour of simulated particles. What sets the Monte Carlo method apart from other ways of solving the neutron transport equation, is that the quantities it actually solves for may be very different. Monte Carlo calculations only provide information for specified quantities being estimated, or tallied, not necessarily the quantities generally present in the transport equation. [4]

By the Monte Carlo method a stochastic process (such as neutron interactions) can be theoretically mimicked. The individual statistical parts of the process are simulated consecutively, while the probability distributions describing these events are sampled stochastically. Sampling is based on random numbers, which is the inspiration for the name "Monte Carlo". [4] Sampling of various quantities is based on known physical phenomena and corresponding probability distribution functions. The principles and techniques of sampling these different quantities are not in the scope of this work and will not be discussed here.

Typically, a Monte Carlo criticality problem is specified by defining the geometry of the system, all involved materials, quantities to be tallied, and some free parameters. The free parameters are the number of active and inactive cycles, the neutron batch size, and the initial fission source distribution. This information is then fed into a Monte Carlo solver, or code, which will iterate a number of generations, or cycles. In every cycle, a number of neutrons, specified as the batch size, is simulated. The inactive cycles are used to converge the guessed initial fission source to a stationary distribution by the Monte Carlo power method. Every active cycle is similarly iterated to obtain estimates for the tallies by sampling neutrons from the fission source distribution, obtained in the preceding cycle.

2.3.1 Non-analog Monte Carlo

Neutron transport is one of the phenomena that can be modelled analogously to the actual process in a natural way. In principle the simplest Monte Carlo neutron transport model is the analog model. In this model natural probabilities of events are used and particles are followed, or tracked, from event to event to accumulate information for tallies. [4]

The so-called analog Monte Carlo neutron transport model is effective when simulated particles contribute significantly to quantities being estimated. However, in

some cases large numbers of particles are simulated that do not partake in accumulating data for specific tallies, increasing their variance. Fortunately, it is possible to use different probability models for neutron transport, which result in the same estimates as the analog model but with lower variance. [21]

In non-analog Monte Carlo algorithms, particles are assigned different importances based on how much they contribute to quantities being tallied. This is done to ensure that the computational effort is spent on simulating particles that are relevant to the results. Any biasing of processes has to be compensated for in order to make sure the results are still correct. If a particle's importance is increased by some factor, its weight has to be decreased accordingly. As estimates are obtained by averaging, this weighting ensures identical results with analog Monte Carlo algorithms. [4]

To illustrate the concept of non-analog Monte Carlo, one can imagine a situation where a quantity is being estimated in a region that only few particles enter. If a particle in this region is then split into, for example, 10 identical particles, each of them contributes to the tally with their contribution weighted by 1/10. Results obtained by analog and non-analog algorithms are equal, however, the non-analog approach provides more statistical samples for the estimate, meaning a lower variance and higher precision. Several so-called variance reduction techniques exist which utilize this principle. [21]

2.3.2 Variance reduction

If one recalls the definition of the figure of merit, as in Eq. (2.36), it becomes understandable how the efficiency of the calculation can be increased by decreasing the variance of estimated quantities. This is true as long as any action taken to decrease variance does not increase the computational time proportionally (or more).

Various variance reduction techniques have been devised that attempt to improve the efficiency and precision of Monte Carlo calculations by decreasing variance. In essence the different techniques can be divided into four categories, described below. [12]

The first type is the truncation methods, which are the simplest variance reduction schemes. Variance is decreased by truncating certain regions of phase-space, which are considered insignificant for the estimation of results. Examples include geometry truncation (parts of geometry are not modelled), time cut-off, and energy cut-off. [12]

The second group consists of population control methods, which utilise particle splitting and a procedure called Russian roulette to control sampling intensity in various parts of phase space. Like in the example given about the non-analog methods, weighting factors are used to specify different importances. Different population control methods are, for example, geometry splitting, energy splitting,

weight cut-off, and weight windows. [21]

The third category consists of modified sampling methods, which are based on changing the statistical sampling in order to increase the number of tallies recorded per particle. Weighting factors are used to un-bias the results, as with previous methods. Available modified sampling methods are quite different from one another. Some examples are exponential transform (or path length stretching), implicit capture, forced collisions, and source biasing. [12]

The last group of variance reduction schemes is partially deterministic methods. These methods partially bypass the normal random walk process by incorporating some deterministic schemes. These are usually the most complex variance reduction methods. This category includes schemes using deterministic transport estimates and methods like correlated sampling. [21]

The big question with variance reduction techniques is always the choice of the correct method. It is not always known which method gives the best results and whether results will actually improve or not. It is also important to remember that a decrease in the estimated variance means higher precision but not necessarily higher accuracy. [13]

Chapter 3

Error analysis of Monte Carlo calculations

> Kalos: *"But in estimating ratios my procedure introduces no bias."*
>
> Gelbard: *"That is where I disagree. I disagree because any estimate you make eventually is based on a normalized eigenvector."*
>
> Kalos: *"But the normalization drops out."*
>
> Gelbard: *"Why does it drop out?"*
>
> EXCERPT FROM [14]

This chapter presents a mathematical description of Monte Carlo criticality calculations. The described notation is then used to identify different aspects of source convergence to explain the problems approached in the thesis. This is followed by error analysis which will be used as a base for work presented later.

3.1 Mathematical description of Monte Carlo criticality calculations

The steady-state homogeneous neutron transport k-eigenvalue, or criticality, equation in operator notation was presented in Eq. (2.21) as

$$k_j T\Phi_j(\mathbf{r}, \mathbf{\Omega}, E) = \frac{\chi(E)}{4\pi} s_j(\mathbf{r})$$

where

$$s_j(\mathbf{r}) = \int_{4\pi}\int_{0}^{\infty} \nu\Sigma_f'\Phi_j(\mathbf{r}, \mathbf{\Omega}', E')\mathrm{d}\mathbf{\Omega}'\mathrm{d}E'$$

In order to find an eigenvalue equation given only by the fission source, firstly, a Green's function is defined as [3]

$$TG(\mathbf{r}_0, \mathbf{\Omega}_0, E_0 \rightarrow \mathbf{r}, \mathbf{\Omega}, E) = \delta(\mathbf{r} - \mathbf{r}_0)\delta(\mathbf{\Omega} - \mathbf{\Omega}_0)\delta(E - E_0) \tag{3.1}$$

where δ is the Dirac's delta function and index 0 denotes the initial point in phase-space. Then the angular flux can be expressed as

$$\Phi_j(\mathbf{r}, \mathbf{\Omega}, E) = \frac{1}{k_j} \int_V \int_{4\pi} \int_0^\infty \frac{\chi_0}{4\pi} s_j(\mathbf{r}_0) G_0 \mathrm{d}\mathbf{r}_0 \mathrm{d}\mathbf{\Omega}_0 \mathrm{d}E_0 \tag{3.2}$$

where $G_0 = G(\mathbf{r}_0, \mathbf{\Omega}_0, E_0 \rightarrow \mathbf{r}, \mathbf{\Omega}, E)$ and $\chi_0 = \chi(E_0)$. For this flux, the fission source can be written as [3]

$$s_j(\mathbf{r}) = \frac{1}{k_j} \int_V \mathrm{d}\mathbf{r}_0 s_j(\mathbf{r}_0) \int_{4\pi} \int_0^\infty \mathrm{d}\mathbf{\Omega}' \mathrm{d}E' \nu\Sigma'_f \int_{4\pi} \int_0^\infty \mathrm{d}\mathbf{\Omega}_0 \mathrm{d}E_0 \frac{\chi_0}{4\pi} G_0 \tag{3.3}$$

Finally, the fission kernel is defined as

$$F(\mathbf{r}_0 \rightarrow \mathbf{r}) = \int_{4\pi} \int_0^\infty \mathrm{d}\mathbf{\Omega}' \mathrm{d}E' \nu\Sigma'_f \int_{4\pi} \int_0^\infty \mathrm{d}\mathbf{\Omega}_0 \mathrm{d}E_0 \frac{\chi_0}{4\pi} G_0 \tag{3.4}$$

which results in the following [3]

$$k_j s_j(\mathbf{r}) = \int_V \mathrm{d}\mathbf{r}_0 F(\mathbf{r}_0 \rightarrow \mathbf{r}) s_j(\mathbf{r}_0) \tag{3.5}$$

By defining an integral operator H for the right hand side, the eigenvalue equation can be written as

$$k_j s_j(\mathbf{r}) = H s_j(\mathbf{r}) \tag{3.6}$$

Monte Carlo calculations solve the criticality equation (3.6) by sampling neutrons from the fission sources and simulating their transport. In each of n iteration cycles a batch of m neutrons are sampled, resulting in a total of mn samples, or neutron histories.

A cycle in the eigenvalue calculation can formally be described as [18]

$$s^{(i+1)} = \frac{1}{k^{(i)}} H s^{(i)} + \epsilon^{(i)} \tag{3.7}$$

where $s^{(i)}$ and $s^{(i+1)}$ are fission sources in consecutive cycles and $\epsilon^{(i)}$ is the stochastic error component resulting from sampling a finite number of histories per cycle. The eigenvalue, $k^{(i)}$, can be estimated as an integral quantity of the fission source

$$k^{(i)} = \frac{\int_V \mathrm{d}\mathbf{r}\, H s^{(i)}(\mathbf{r})}{\int_V \mathrm{d}\mathbf{r}\, s^{(i)}(\mathbf{r})} \tag{3.8}$$

Fission sources are normalized to the batch size m, i.e.

$$\int_V \mathrm{d}\mathbf{r}\, s^{(i)}(\mathbf{r}) = m \tag{3.9}$$

The estimates of quantities are then calculated as averages of obtained cycle-wise values. For any quantity x, the estimate of n cycles is calculated as

$$\left\langle x^{(n)} \right\rangle = \frac{1}{n} \sum_{i=1}^{n} x^{(i)} \tag{3.10}$$

where $x^{(i)}$ is the i^{th} cycle estimate of x.

3.2 Aspects of fission source convergence

It is characteristic for Monte Carlo calculations that the combined results contain errors of statistical sampling of the order $O(1/\sqrt{mn})$, with mn being the total number of neutron histories simulated over the cycles. [20] For any Monte Carlo process it is assumed that $\mathrm{E}[\epsilon^{(i)}] = 0$. [18] This means that statistical errors are decreased by increasing the number of samples, and if there were no systematic errors in the computational scheme, overall errors would be decreased accordingly.

The process of solving the eigenvalue equation, as given in Eq. (3.7), is described as an iterative process, very much like the power method. If the iterations are followed from the first to the n^{th} cycle, the fission source can be written as

$$s^{(n)} = \frac{H^n s^{(0)}}{\prod_{j=1}^{n} k^{(j-1)}} + \sum_{j=1}^{n} \frac{H^{n-j} \epsilon^{(j-1)}}{\prod_{l=j}^{n} k^{(l)}} \tag{3.11}$$

Keeping in mind Eq. (3.6), any fission source distribution can be expressed as a sum of eigenfunctions, using some arbitrary weighting factors (a_j-s and c)

$$s^{(n)} = H^n \sum_j a_j s_j + c\,\epsilon^{(n)} = \sum_j a_j k_j^n s_j + c\,\epsilon^{(n)} \tag{3.12}$$

To proceed, the eigenvalues are ordered descendingly by the modulus, starting with the highest value ($k_0 > |k_1| > |k_2| > \ldots$). The equation above can then be divided by k_0^n to obtain

$$\frac{s^{(n)}}{k_0^n} = a_0 s_0 + \left(\frac{k_1}{k_0}\right)^n a_1 s_1 + \left(\frac{k_2}{k_0}\right)^n a_2 s_2 + \ldots + c\,\epsilon^{(n)} \tag{3.13}$$

Based on the ordering of eigenvalues, it can be seen that the iterations converge to a multiple of the fundamental mode eigenvector plus the remaining statistical error (which decays as $\sqrt{mn}$ increases), and

$$1 > |k_1/k_0| > |k_2/k_0| > \ldots$$

It becomes apparent that convergence of such a calculation is governed by k_1/k_0, also known as the dominance ratio. More precisely, as Eq (3.13) shows, the convergence rate is related to $(k_1/k_0)^n$, which shows a dependence on the number of cycles.

It has also been shown that convergence of the Monte Carlo fission source to a multiple of the correct eigenvector is, in fact, governed by the dominance ratio. [34, 35] This fact plays an important role in source convergence in systems with dominance ratios close to one.

What is more, it has been long known that the results of Monte Carlo eigenvalue calculations also contain systematic errors. [13, 14] The magnitude of these errors, known as biases, have been shown to be of the order $O(1/m)$. [1, 6, 11, 18, 38] By definition, the bias in the Monte Carlo estimate of the fundamental mode eigenvector is [18]

$$\Delta s_0 = s_0^* - s_0 = \left\langle \frac{1}{m} s^{(i)} \right\rangle - s_0 \tag{3.14}$$

where s_0 is the correct fundamental mode eigenvector of Eq. (3.18) and s_0^* is the biased estimate, both normalised to identity. The definition of bias is based on the assumption that the calculation has converged and the statistical errors have become negligible. An example of a biased eigenvector can be seen in Fig. 3.1, where it has been calculated with different batch sizes. Following suit, the eigenvalue bias is defined as

$$\Delta k_0 = k_0^* - k_0 = \left\langle k^{(i)} \right\rangle - k_0 \tag{3.15}$$

where asterisk denotes a biased quantity, like above. [18]

It has been shown how to quantify the eigenvalue bias based on the real and estimated variances. [1] The Brissenden–Garlick relation gives the eigenvalue bias as

$$\Delta k_0 = -\frac{n}{2k_0} \left(\sigma_R^2 - \sigma_S^2 \right) \tag{3.16}$$

but the problem of calculating the source bias has remained open. Nevertheless, more can be learnt about it by analysing cycle-wise error propagation, as presented in the next section.

Considering the existence of the discussed biases, it is natural that relatively larger batch sizes are preferred. [2] However, it must be kept in mind that the product of the batch size and number of cycles determines the total number of histories simulated, which is a finite value limited by available computational time. This means a large batch size limits the number of cycles that are simulated, meaning the error originating from the initial fission source may not decrease enough, corrupting the calculation results. It follows that for any Monte Carlo criticality calculation, there is an optimal neutron batch size to balance these two effects.

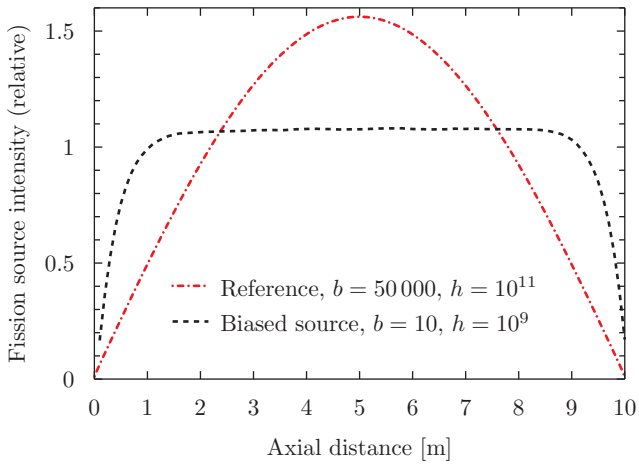

Figure 3.1: Two fission source distributions computed for the same system with different batch sizes. The very low batch size has caused a significant bias in the fission source. The studied system is a 10 m long fuel rod surrounded by water, with void boundary conditions set in axial and reflective in radial direction.

3.3 Errors in the Monte Carlo fission source

The analysis of Monte Carlo eigenvalue calculations is often simplified by using discrete phase-space notation. [15, 16, 18] This is a notation, where the system is divided into spatial regions, also known as cells. If these cells are infinitesimally small, the discrete model is equivalent to the continuous. [3] This approach makes it possible to describe the calculation using simpler notation.

Assuming the aforementioned discretisation, the operator in the eigenvalue equation can be described as a matrix, here called the fission matrix. [5] Following suit, the fission source in the system is represented as a vector. In this fission source vector, each element specifies the number of fission neutrons in the corresponding box of the discretised phase-space. [18]

Elements of the fission matrix can be expressed as [5]

$$\mathbf{H}_{i,j} = \frac{\int\limits_{\mathbf{r}\in \mathrm{Z}_i} \mathrm{d}\mathbf{r} \int\limits_{\mathbf{r}_0\in \mathrm{Z}_j} \mathrm{d}\mathbf{r}_0 F(\mathbf{r}_0 \to \mathbf{r}) s_0(\mathbf{r}_0)}{\int\limits_{\mathbf{r}_0\in \mathrm{Z}_j} \mathrm{d}\mathbf{r}_0\, s_0(\mathbf{r}_0)} \tag{3.17}$$

The $(i,j)^{\mathrm{th}}$ element of $\mathbf{H}$ represents the number of neutron births in space zone i, caused by a fission neutron born in space zone j. Some of the Monte Carlo codes have a built-in capability to calculate the fission matrix during standard Monte Carlo calculations (e.g. TRIPOLI-4 [27] or KENO V.a [30]).

In the described notation, the eigenvalue equation (3.6) is transformed into

$$\mathbf{H}\mathbf{s}_j = k_j \mathbf{s}_j \tag{3.18}$$

where $\mathbf{H}$ is the fission matrix and $\mathbf{s}_j$ is the vector analog of $s_j(\mathbf{r})$. The cycles simulated to solve this equation can then be modelled as

$$\mathbf{s}^{(i+1)} = \frac{\mathbf{H}\mathbf{s}^{(i)}}{k^{(i)}} + \boldsymbol{\epsilon}^{(i)} \tag{3.19}$$

which is the discrete space analog of Eq. (3.7) with $\mathbf{s}^{(i)}$ as the fission source vector. An integral operator is defined as a row vector $\boldsymbol{\tau} = (1, 1, \ldots, 1)$ so that

$$\boldsymbol{\tau}\mathbf{s}^{(i)} = \int_V \mathrm{d}\mathbf{r}\, s^{(i)}(\mathbf{r}) = m \tag{3.20}$$

Based on this, the eigenvalue is calculated as

$$k^{(i)} = \frac{\boldsymbol{\tau}\mathbf{H}\mathbf{s}^{(i)}}{\boldsymbol{\tau}\mathbf{s}^{(i)}} = \frac{\boldsymbol{\tau}\mathbf{H}\mathbf{s}^{(i)}}{m} \tag{3.21}$$

which is the discrete space equivalent of Eq. (3.8).

The fission source distribution is one of the fundamental quantities in Monte Carlo calculations. Like the eigenvalue, other quantities can be calculated from it. This is why the mathematical description is centered around the fission source and the errors in it will be studied further. The fission source error in cycle i is introduced as

$$\mathbf{e}^{(i)} = \mathbf{s}^{(i)} - m\,\mathbf{s}_0 \tag{3.22}$$

In order to analyse such error vectors, Eq. (3.22) is substituted into (3.19) to produce

$$\mathbf{e}^{(i+1)} = \frac{m\mathbf{H}\left(m\,\mathbf{s}_0 + \mathbf{e}^{(i)}\right)}{\boldsymbol{\tau}\mathbf{H}\left(m\,\mathbf{s}_0 + \mathbf{e}^{(i)}\right)} - m\,\mathbf{s}_0 + \boldsymbol{\epsilon}^{(i)} \tag{3.23}$$

This can be rearranged into

$$\mathbf{e}^{(i+1)} = \frac{1}{1 + \dfrac{\boldsymbol{\tau}\mathbf{H}\mathbf{e}^{(i)}}{m\boldsymbol{\tau}\mathbf{H}\mathbf{s}_0}} \left[\frac{\mathbf{H}\left(m\,\mathbf{s}_0 + \mathbf{e}^{(i)}\right)}{\boldsymbol{\tau}\mathbf{H}\mathbf{s}_0}\right] - m\,\mathbf{s}_0 + \boldsymbol{\epsilon}^{(i)} \tag{3.24}$$

Based on the identity $\dfrac{1}{1+x} = 1 - x + x^2 - x^3 + \ldots$, it is expanded in series as

$$\mathbf{e}^{(i+1)} = \sum_{j=0}^{\infty} \left(-\frac{\boldsymbol{\tau}\mathbf{H}\mathbf{e}^{(i)}}{k_0 m\boldsymbol{\tau}\mathbf{s}_0}\right)^j \left[\frac{\mathbf{H}\left(m\,\mathbf{s}_0 + \mathbf{e}^{(i)}\right)}{k_0\boldsymbol{\tau}\mathbf{s}_0}\right] - m\,\mathbf{s}_0 + \boldsymbol{\epsilon}^{(i)} \tag{3.25}$$

The fundamental mode eigenvector is normalised to one as $\boldsymbol{\tau}\mathbf{s}_0 = 1$. The first terms of the expansion are written as

$$\mathbf{e}^{(i+1)} = m\,\mathbf{s}_0 + \frac{\mathbf{H}\mathbf{e}^{(i)}}{k_0} - \frac{\mathbf{s}_0\boldsymbol{\tau}\mathbf{H}\mathbf{e}^{(i)}}{k_0} - \frac{\mathbf{H}\mathbf{e}^{(i)}\boldsymbol{\tau}\mathbf{H}\mathbf{e}^{(i)}}{k_0^2 m} + \frac{\mathbf{s}_0\boldsymbol{\tau}\mathbf{H}\mathbf{e}^{(i)}\boldsymbol{\tau}\mathbf{H}\mathbf{e}^{(i)}}{k_0^2 m} + \\ + O(m^{-2}) - m\,\mathbf{s}_0 + \boldsymbol{\epsilon}^{(i)} \tag{3.26}$$

Next, an operator—the noise propagation matrix—is formed by combining some of the terms in the expansion, so that

$$\mathbf{A} = \frac{\mathbf{I} - \mathbf{s}_0\boldsymbol{\tau}}{k_0}\mathbf{H} \tag{3.27}$$

where $\mathbf{I}$ is the identity matrix. Keeping in mind the knowledge that biases are of the order $O(1/m)$, the terms of the order $O(1/m^2)$ and smaller are disregarded. [1, 18] This yields

$$\mathbf{e}^{(i+1)} \cong \mathbf{A}\mathbf{e}^{(i)} - \frac{\boldsymbol{\tau}\mathbf{H}}{k_0 m}\mathbf{e}^{(i)}\mathbf{A}\mathbf{e}^{(i)} + \boldsymbol{\epsilon}^{(i)} \tag{3.28}$$

A more widely used error propagation equation (as seen in the works of Ueki, Sutton, Nease, and others [25, 32, 33]) is obtained when a simpler, linear approximation is taken

$$\tilde{\mathbf{e}}^{(i+1)} \cong \mathbf{A}\tilde{\mathbf{e}}^{(i)} + \boldsymbol{\epsilon}^{(i)} \tag{3.29}$$

Returning to the bias, it can be analysed by looking at the ensemble average value of Eq. (3.28). After sufficiently many cycles n it can be assumed that the process is stationary, noted by $\langle\mathbf{e}^{(n)}\rangle \cong \langle\mathbf{e}^{(n-1)}\rangle$. [18] This way Eq. (3.28) yields

$$\left\langle \mathbf{e}^{(n)} \right\rangle = -\frac{(\mathbf{I} - \mathbf{A})^{-1}}{k_0 m}\mathbf{A}\left\langle \mathbf{e}^{(n)}\mathbf{e}^{(n)\mathsf{T}} \right\rangle \mathbf{H}^{\mathsf{T}}\boldsymbol{\tau}^{\mathsf{T}} \tag{3.30}$$

which shows that the iteration converges to a non-zero value—the bias. [18]

In addition to the error vector specified in Eq. (3.22), the relative error in one cycle is defined as the error normalised to one neutron

$$\boldsymbol{\varepsilon}^{(i)} = \frac{\mathbf{e}^{(i)}}{m} = \frac{\mathbf{s}^{(i)}}{m} - \mathbf{s}_0 \tag{3.31}$$

To make these errors more easily quantifiable, any scalar relative error is defined as the norm of the respective relative error vector

$$\varepsilon = \|\boldsymbol{\varepsilon}\| \tag{3.32}$$

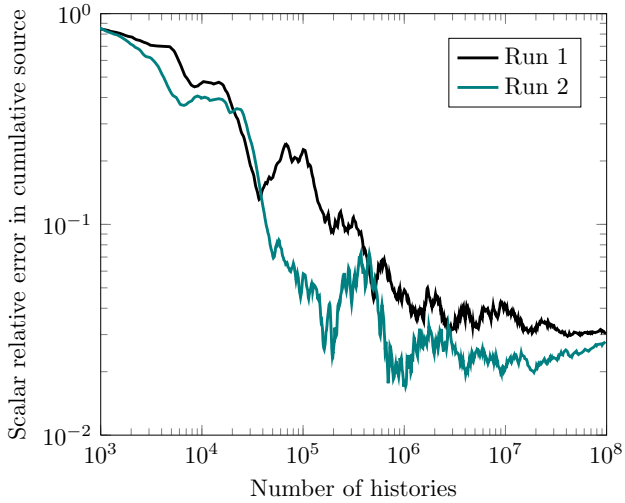

Figure 3.2: Changes of relative error in the cumulative fission source over the number of histories in two example calculations with a batch size of 100 neutrons. The studied system is a 4 m long fuel rod surrounded by water, with void boundary conditions set in axial and reflective in radial direction.

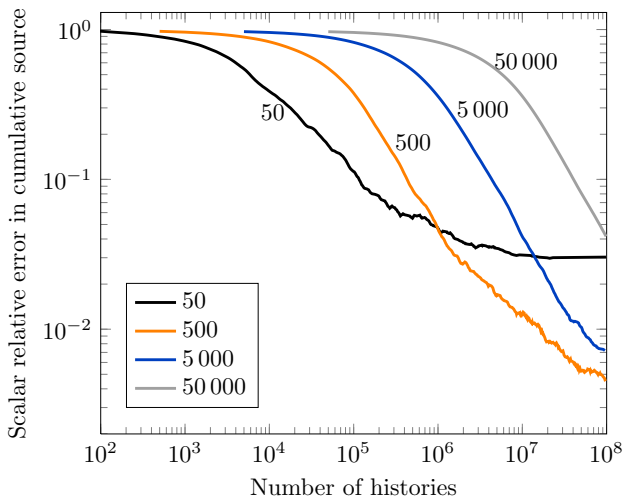

Figure 3.3: Comparison of errors in calculations with different neutron batch sizes. Batches of 50, 500, 5 000, and 50 000 neutrons were used; all calculations were repeated 40 times and results averaged. Calculations were made on the same system as in Fig. 3.2.

If the relative errors are averaged over n cycles, the relative error in the fission source that is combined over the cycles can be found as

$$\bar{\varepsilon} = \left\langle \boldsymbol{\varepsilon}^{(n)} \right\rangle = \frac{1}{n} \sum_{i=1}^{n} \boldsymbol{\varepsilon}^{(i)} = \frac{1}{mn} \sum_{i=1}^{n} \mathbf{e}^{(i)} \tag{3.33}$$

It can also be seen that by definition the relative error in the cumulative fission source is equal to the eigenvector bias when the calculation has become stationary. In other words, the relative error decays into the bias in conditions matching its definition (i.e. no other errors are remaining).

Direct calculation of these errors is presented in Ch. 4, where it can be seen that this kind of relative error estimate captures the presence of fission source bias and errors coming from the initial source. This is also illustrated in Figs. 3.2 and 3.3. The first figure shows changes in the relative error of the cumulative fission source in two individual Monte Carlo calculations and the second shows the decrease of the relative error in averaged results of repeated calculations with different batch sizes. Both the decrease of the initial error and reaching the bias can be seen.

3.4 Notes about the noise propagation matrix and fission matrix

It has been shown that the highest modulus eigenvalue of the noise propagation matrix (NPM) corresponds to the dominance ratio of the system, however, in somewhat different mathematical notation than used in this work. [23, 26]

It can be verified that the vector notation used in this work is equivalent to the notation used by Ueki et al. [23, 26, 32] This is done in order to make sure that the eigenvalues of the noise propagation matrix correspond to k_j/k_0 ratios of the fission matrix (or the transport equation).

If Eq. (3.19) is multiplied by $k^{(i)}\mathbf{s}^{(i)\mathsf{T}}$ from the right, it can be rearranged as

$$k^{(i)}\mathbf{s}^{(i+1)}\mathbf{s}^{(i)\mathsf{T}} = \mathbf{H}\mathbf{s}^{(i)}\mathbf{s}^{(i)\mathsf{T}} + k^{(i)}\boldsymbol{\epsilon}^{(i)}\mathbf{s}^{(i)\mathsf{T}} \tag{3.34}$$

Next, the mean of this equation is taken

$$\mathbf{H}\left\langle \mathbf{s}^{(n)}\mathbf{s}^{(n)\mathsf{T}} \right\rangle = \left\langle k^{(n)}\mathbf{s}^{(n+1)}\mathbf{s}^{(n)\mathsf{T}} \right\rangle - \left\langle k^{(n)}\boldsymbol{\epsilon}^{(n)}\mathbf{s}^{(n)\mathsf{T}} \right\rangle \tag{3.35}$$

Assuming $\left\langle \boldsymbol{\epsilon}^{(n)}\mathbf{e}^{(n)\mathsf{T}} \right\rangle = \mathbf{0}$, it is equivalent to [25]

$$\mathbf{H}\left\langle \mathbf{s}^{(n)}\mathbf{s}^{(n)\mathsf{T}} \right\rangle = \left\langle k^{(n)} \right\rangle \left\langle \mathbf{s}^{(n+1)}\mathbf{s}^{(n)\mathsf{T}} \right\rangle \tag{3.36}$$

from this, the fission matrix is expressed as

$$\mathbf{H} = \bar{k}\,\mathbf{L'}_1\mathbf{L'}_0^{-1} \tag{3.37}$$

where $\bar{k} = \langle k^{(n)} \rangle$ and the source correlation matrices $\mathbf{L'}_0$ and $\mathbf{L'}_1$ are defined as

$$\begin{aligned} \mathbf{L'}_0 &= \left\langle \mathbf{s}^{(n)} \mathbf{s}^{(n)\mathsf{T}} \right\rangle \\ \mathbf{L'}_1 &= \left\langle \mathbf{s}^{(n+1)} \mathbf{s}^{(n)\mathsf{T}} \right\rangle \end{aligned} \tag{3.38}$$

using notation consistent with [23]. Interestingly, this can be used to show

$$\mathbf{L'}_1 \mathbf{L'}_0^{-1} \mathbf{s}_j = \frac{k_j}{\bar{k}} \mathbf{s}_j \tag{3.39}$$

From the definition of the NPM

$$\mathbf{A} = \frac{\bar{k}}{k_0} \left(\mathbf{I} - \mathbf{s}_0 \boldsymbol{\tau} \right) \mathbf{L'}_1 \mathbf{L'}_0^{-1} \tag{3.40}$$

Assuming no biasing, i.e. $\bar{k} = k_0$

$$\mathbf{A} = \left(\mathbf{I} - \mathbf{s}_0 \boldsymbol{\tau} \right) \mathbf{L'}_1 \mathbf{L'}_0^{-1} \tag{3.41}$$

which is equivalent to the result in [32]

$$\mathbf{A} = \left(\mathbf{L'}_1 - \mathbf{s}\mathbf{s}^{\mathsf{T}} \right) \mathbf{L'}_0^{-1} \tag{3.42}$$

where $\mathbf{s} = m\mathbf{s}_0$. This is enough to ensure that the noise propagation matrix is equivalent in both notations. The equations above also offer a derivation for the NPM that is not affected by the simplifications made in Eq.(3.29), which has hitherto been used for this purpose.

What is more, Eq. (3.37) offers a different kind of expression for the fission matrix, which can be evaluated very similarly to the NPM as suggested by Sutton et al. [32] It has been shown that the NPM method is not sensitive to mesh sizing, [32] unlike the fission matrix. [24] The fission matrix in Eq. (3.37) can be expected to be affected by biased fission sources, however, it is possibly less influenced by spatial meshing than the traditional way of evaluating the fission matrix. [9, 10] In addition to that, Eq. (3.39) shows that the dominance ratio, or higher mode eigenpairs, can also be calculated from the source correlation matrices.

Chapter 4

Estimation of errors in the cumulative fission source

This chapter describes a way of estimating the scalar error in the cumulative Monte Carlo fission source. It is known that the fission matrix can be estimated accurately even with a small batch size if the spatial zones are sufficiently small. This suggests that it may be possible to estimate the errors in the cumulative source based on the fundamental mode eigenvector of the fission matrix. This method was published in Paper 1.

4.1 Fission matrix eigenvector method

It has been shown that the fission matrix becomes less sensitive to errors in the fission source as the mesh zones are decreased. [9] Hence, the errors in the fission source become irrelevant for sampling the fission matrix when the zones are small enough. This means that the fission matrix and its fundamental-mode eigenvector can be correctly evaluated during a Monte Carlo criticality calculation even if the fission source is biased.

What is more, it has been observed that fission matrix based criticality calculations converge faster than standard Monte Carlo criticality calculations, i.e. the eigenvector of the matrix converges faster than the cumulative fission source. [5, 9] These qualities of the fission matrix eigenvector can be utilised in estimating the error in the cumulative fission source.

The relative error $\bar{\boldsymbol{\varepsilon}}$ in the cumulative fission source is defined as

$$\bar{\boldsymbol{\varepsilon}} = \mathbf{s}_c - \mathbf{s}_0 \tag{4.1}$$

where $\mathbf{s}_c$ is the cumulative fission source and $\mathbf{s}_0$ the correct fundamental mode eigenvector of the system, both normalised to one (i.e. $\boldsymbol{\tau}\mathbf{s}_c = \boldsymbol{\tau}\mathbf{s}_0 = 1$). The

relative scalar error is then

$$\bar{\varepsilon} = \|\mathbf{s}_c - \mathbf{s}_0\|_1 = \sum_i |\bar{\varepsilon}_i| \tag{4.2}$$

where the one-norm is defined as

$$\|\mathbf{x}\|_1 = \sum_i |x_i|.$$

The fundamental-mode source $\mathbf{s}_0$ is unknown and the correct value of $\bar{\varepsilon}$ cannot be computed. However, it is proposed that its value can be estimated as

$$\hat{\varepsilon} = \|\mathbf{s}_c - \mathbf{q}\|_1 \tag{4.3}$$

where $\mathbf{q}$ is the eigenvector of the fission matrix $\mathbf{H}$ that was sampled over the same cycles as the cumulative fission source $\mathbf{s}_c$ (also normalised to one as $\boldsymbol{\tau}\mathbf{q} = 1$).

The fission matrix $\mathbf{H}$ can be expected to contain random errors of the order $O(1/\sqrt{nm})$ that must also be present in its eigenvector $\mathbf{q}$. The errors in $\mathbf{q}$ are denoted by the vector $\boldsymbol{\delta}$, so that

$$\boldsymbol{\delta} = \mathbf{q} - \mathbf{s}_0 \tag{4.4}$$

Then, Eq. (4.3) can be written as

$$\hat{\varepsilon} = \|\bar{\boldsymbol{\varepsilon}} - \boldsymbol{\delta}\|_1 \tag{4.5}$$

or in another way

$$\hat{\varepsilon} = \sum_i |\bar{\varepsilon}_i - \delta_i| \tag{4.6}$$

Here it has to be noted that $\bar{\boldsymbol{\varepsilon}}$ contains statistical errors, the bias, and the partly decayed errors coming from the initial fission source.

Since both $\mathbf{q}$ and $\mathbf{s}_0$ are normalised to unity, it can be written that

$$\sum_i |q_i| = \sum_i |s_{0\,i}| \tag{4.7}$$

which is equivalent to

$$\sum_i (|q_i| - |s_{0\,i}|) = 0 \tag{4.8}$$

Since all elements in $\mathbf{q}$ and $\mathbf{s}_0$ are non-negative, the absolute value signs in Eq. (4.8) can be removed,

$$\sum_i (q_i - s_{0\,i}) = 0 \tag{4.9}$$

which is equivalent to

$$\sum_i \delta_i = 0 \tag{4.10}$$

Hence, the vector $\boldsymbol{\delta}$ must contain both positive and negative elements so that their sum would equal zero. This quality of $\boldsymbol{\delta}$ suggests that the expected value of $\hat{\varepsilon}$ equals

$$\mathrm{E}(\hat{\varepsilon}) = \sum_i |\bar{\varepsilon}_i| = \bar{\varepsilon} \tag{4.11}$$

assuming that $\boldsymbol{\delta}$ and $\bar{\boldsymbol{\varepsilon}}$ are not correlated. Hence, if this condition is satisfied then the error estimate $\hat{\varepsilon}$ given by Eq. (4.3) is normally distributed around $\bar{\varepsilon}$. It is, however, not apparent whether this condition is satisfied or not.

4.2 Test calculations

4.2.1 Test model

Numerical test calculations were performed on a fuel pin cell with parameters summarised in Table 4.1. Reflective boundary conditions were applied to radial surfaces and void boundary conditions to axial faces. This model is based on a common PWR fuel pin cell, with the pin length increased to 10 m in order to achieve a high dominance ratio. All numerical calculations were performed by an in-house non-analog continuous-energy 3D Monte Carlo criticality code using the JEFF3.1 point-wise neutron cross-section library.

Table 4.1: Specifications of the test model.

Fuel	UO_2
Cladding material	Zr
Moderator	light water
Radius of fuel pellets	0.41 cm
Outer radius of cladding	0.475 cm
Rod pitch	1.26 cm
Length of the fuel rod	1000 cm
^{235}U enrichment	3.1 wt%
Fuel density	10 g/cm^3
Moderator (water) density	0.7 g/cm^3

An analytical fundamental mode fission source is not known and is thus estimated by a reference calculation. Parameters of the reference calculation are summarised in Table 4.2. The reference distribution of the fission source, $\mathbf{s}_{\mathrm{ref}}$, was evaluated using a fine uniform mesh with 100 axial zones, and combined over all active cycles. As the test model is axially symmetrical, the accuracy of $\mathbf{s}_{\mathrm{ref}}$ has further been improved by symmetrising it. During the reference calculation, the dominance ratio of the test model was evaluated to be 0.9982 from the sampled fission matrix.

Table 4.2: Reference calculation.

Neutron batch size	50 000
Number of active cycles	2 000 000
Number of inactive cycles	2000
Initial fission source	flat

Table 4.3 specifies the test calculations (A-D). While the neutron batch size varied in calculations A-D, all calculations simulated 10^9 neutron histories. The initial fission source was randomly sampled from a uniform distribution in the first cycle of each calculation. In each calculation, the fission matrix was sampled over all cycles; no cycles were skipped.

Table 4.3: Parameters of test cases A-D.

Calculation	A	B	C	D
Neutron batch size	50	500	5000	50 000
Number of neutron histories			1 billion	

For the purpose of the test calculations, the axial dimension of all zones are set to 10 cm; hence, the fission matrix is evaluated on a spatial mesh with 100 zones. This mesh appears sufficient for eliminating the bias in the fission matrix (that could possibly arise from the biased fission source). This is demonstrated in Fig. 4.1 which compares the eigenvector of the fission matrix to the cumulative fission source biased by the batch size of 50 neutrons; the fission matrix was sampled by the actual biased fission source. While the fission source is strongly biased, the eigenvector of the fission matrix is close to the reference solution in Fig. 4.1.

In calculations A-D, the real relative error ε in the cumulative fission source distribution $\mathbf{s}_\mathrm{c}$ is evaluated as

$$\varepsilon = \left\| \tilde{\mathbf{s}}_\mathrm{c} - \tilde{\mathbf{s}}_\mathrm{ref} \right\|_1 . \tag{4.12}$$

The estimation $\hat{\varepsilon}$ of the relative error in a cumulative fission source is computed according to Eq. (4.3).

4.2.2 Results

The values of $\hat{\varepsilon}$ and ε obtained from all the test cases are compared in Tables 4.4–4.7. In each calculation, the values of $\hat{\varepsilon}$ and ε are calculated at several stages, always after simulating 10^6, 10^7, 10^8 and 10^9 neutron histories. To associate a certain value of $\hat{\varepsilon}$ or ε to a certain stage, we add a superscript in square brackets to $\hat{\varepsilon}$ and ε, denoting the number of simulated neutron histories; e.g., the values of $\hat{\varepsilon}^{[10^9]}$ and $\varepsilon^{[10^9]}$ are computed after simulating 10^9 neutron histories.

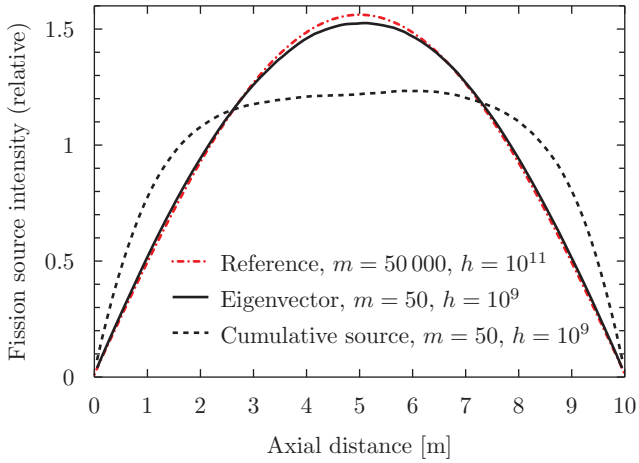

Figure 4.1: Comparison of the reference solution, the eigenvector of a fission matrix sampled by a biased fission source, and the biased fission source obtained with the batch size $m = 50$.

Results from calculation A (with the batch size of 50 neutrons) are summarised in Table 4.4. As the bias in the fission source is large due to the small neutron batch size (as depicted in Fig. 3.1), $\varepsilon^{[10^7]}$, $\varepsilon^{[10^8]}$ and $\varepsilon^{[10^9]}$ remain about equally large, close to 20%. This is correctly captured by the corresponding values of $\hat{\varepsilon}^{[10^7]}$, $\hat{\varepsilon}^{[10^8]}$ and $\hat{\varepsilon}^{[10^9]}$. The value of $\hat{\varepsilon}^{[10^6]}$ is less than half of that of $\varepsilon^{[10^6]}$; in this case, the relatively large random errors in the eigenvector of fission matrix (that was sampled by only 10^6 neutron histories) decreased the estimated error.

Table 4.4: Comparison of ε and $\hat{\varepsilon}$ in calculation A (with the batch size of **50** neutrons) [%].

h (# of neutron histories)	$\varepsilon^{[h]}$	$\hat{\varepsilon}^{[h]}$
10^6	36.7	14.9
10^7	18.3	18.4
10^8	18.1	18.2
10^9	20.2	18.6

Results from calculation B (with the batch size of 500 neutrons) are summarised in Table 4.5. Here, values of $\hat{\varepsilon}$ also correspond well to ε, with the exception of the value of $\hat{\varepsilon}^{[10^8]}$ that underestimated the real error several times.

Results from calculation C (with the batch size of 5000 neutrons) are summarised in Table 4.6. This case shows that $\hat{\varepsilon}$ may overestimate the real error several times as well; note the value of $\hat{\varepsilon}^{[10^6]}$ and $\hat{\varepsilon}^{[10^7]}$. The small bias in the cumulative fission

Table 4.5: Comparison of ε and $\hat{\varepsilon}$ in calculation B (with the batch size of **500** neutrons) [%].

h (# of neutron histories)	$\varepsilon^{[h]}$	$\hat{\varepsilon}^{[h]}$
10^6	24.0	19.8
10^7	12.4	8.21
10^8	3.78	1.10
10^9	4.53	3.63

source combined over 10^9 neutron histories was correctly estimated.

Table 4.6: Comparison of ε and $\hat{\varepsilon}$ in calculation C (with the batch size of **5000** neutrons) [%].

h (# of neutron histories)	$\varepsilon^{[h]}$	$\hat{\varepsilon}^{[h]}$
10^6	17.7	41.0
10^7	8.23	18.3
10^8	8.41	6.44
10^9	1.17	1.25

Results from calculation D (with the batch size of 50 000 neutrons) are summarised in Table 4.7. In this case, $\hat{\varepsilon}$ estimated the real error in the cumulative fission source in all stages of the calculation with a good accuracy.

Table 4.7: Comparison of ε and $\hat{\varepsilon}$ in calculation D (with the batch size of **50 000** neutrons) [%].

h (# of neutron histories)	$\varepsilon^{[h]}$	$\hat{\varepsilon}^{[h]}$
10^6	37.9	28.2
10^7	26.1	25.1
10^8	4.51	4.29
10^9	1.15	1.25

It should be noted that the above results depend on the initial seed of the RNG; as such, $\hat{\varepsilon}$ is a random variable. Repeating the identical calculation with another seed would produce different results (both $\hat{\varepsilon}$ and ε). Nevertheless, the above results suggest clearly that $\hat{\varepsilon}$ can be used in estimating the order of magnitude of the error in the cumulative fission source.

4.3 Conclusions

The fact that the fission matrix can be well sampled even by a biased or not fully converged Monte Carlo fission source can be utilised for various purposes. In this chapter, the possibility of using the fundamental-mode eigenvector of the fission matrix for estimating the error in the cumulative fission source was analysed. The work also attempted to establish if the random errors, that are naturally present in the eigenvector, hinder the estimation of the error in the cumulative fission source.

It can be concluded that the estimation of the error in the cumulative fission source obtained from the eigenvector of the fission matrix is distributed around the real error, assuming that the random errors in the eigenvector and the cumulative fission source are not correlated. However, the validity of this assumption is not completely apparent. Nevertheless, the numerical test calculations confirmed the error estimates were distributed around the real errors, which suggests the errors are either not correlated or the correlation is weak. The error estimations correctly captured the presence of the source bias, as well as the source errors coming from the initial fission source.

Chapter 5

Simplified error model and STORM

"Everything that can be optimised, should be optimised, and what cannot be optimised, should be made optimisable."

Prof. Mati Valdma

Efficiency of the calculation can be improved by maximising the figure of merit. In this work, the figure of merit is based on a simplified estimate of the error in the cumulative fission source (the fission source combined over all simulated cycles). An equation is derived that relates this error to the neutron batch size, total number of histories, dominance ratio of the system, and the relative error committed by guessing the initial fission source. Knowing how the figure of merit is affected by the choice of batch size allows its value to be optimised. This work was presented in Paper 2.

5.1 Derivation of simplified error model

First of all, the error vector is decomposed into three components

$$\mathbf{e}^{(i)} = \mathbf{e}_A^{(i)} + \mathbf{e}_B^{(i)} + \mathbf{e}_R^{(i)} \tag{5.1}$$

where the first term describes the decay of the error coming from the initial fission source, the second term includes the bias, and the third term is the stochastic error component.

Based on earlier definitions, the scalar relative error in cycle i is expressed as

$$\varepsilon^{(i)} = \|\boldsymbol{\varepsilon}^{(i)}\| = \|\boldsymbol{\varepsilon}_A^{(i)} + \boldsymbol{\varepsilon}_B^{(i)} + \boldsymbol{\varepsilon}_R^{(i)}\| \tag{5.2}$$

By properties of norms, the value on the right hand side has an upper bound of

$$\|\boldsymbol{\varepsilon}_A^{(i)} + \boldsymbol{\varepsilon}_B^{(i)} + \boldsymbol{\varepsilon}_R^{(i)}\| \leq \|\boldsymbol{\varepsilon}_A^{(i)}\| + \|\boldsymbol{\varepsilon}_B^{(i)}\| + \|\boldsymbol{\varepsilon}_R^{(i)}\| \tag{5.3}$$

so that

$$\varepsilon^{(i)} \leq \varepsilon_A^{(i)} + \varepsilon_B^{(i)} + \varepsilon_R^{(i)} \tag{5.4}$$

which implies

$$\bar{\varepsilon} \leq \bar{\varepsilon}_A + \bar{\varepsilon}_B + \bar{\varepsilon}_R \tag{5.5}$$

for the relative error in the cumulative fission source.

Eq. (5.1) was specified so that the $\mathbf{e}_B^{(i)}$ component describes the bias; thus, when the calculation has become stationary, it can be expressed as

$$\bar{\boldsymbol{\varepsilon}}_B = \Delta\mathbf{s}_0 = \left\langle \frac{\mathbf{e}^{(n)}}{m} \right\rangle \tag{5.6}$$

Based on that and Eq. (3.30), it is continued as

$$\bar{\boldsymbol{\varepsilon}}_B = -\frac{1}{m} \left(\mathbf{I} - \mathbf{A}\right)^{-1} \mathbf{A} \left\langle \frac{\mathbf{e}^{(n)}\mathbf{e}^{(n)\mathsf{T}}}{m} \right\rangle \frac{\mathbf{H}^{\mathsf{T}}\boldsymbol{\tau}^{\mathsf{T}}}{k_0} \tag{5.7}$$

It is possible to show that this component is in fact of the order $O(1/m)$, as it would be expected from the bias.

As the fundamental mode eigenvalue of the noise propagation matrix is equivalent to the dominance ratio of the system, it is known that the spectral radius of the noise propagation matrix is less than one, allowing the inverse to be written as a Neumann series

$$\left(\mathbf{I} - \mathbf{A}\right)^{-1} = \sum_{j=0}^{\infty} \mathbf{A}^j \tag{5.8}$$

From the definition of cycle-wise error it follows that

$$\mathbf{A} \left\langle \frac{\mathbf{e}^{(n)}}{m} \right\rangle = \mathbf{A}\mathbf{s}_0^*$$

and

$$\left\langle \mathbf{e}^{(n)\mathsf{T}} \right\rangle \mathbf{H}^{\mathsf{T}}\boldsymbol{\tau}^{\mathsf{T}} = m\Delta k_0$$

The norm can then be expressed as

$$\|\bar{\boldsymbol{\varepsilon}}_B\| \leq \left| -\frac{1}{m} \right| \left\| \sum_{j=1}^{\infty} \mathbf{A}^j \mathbf{s}_0^* \right\| \left| \frac{m\Delta k_0}{k_0} \right| \tag{5.9}$$

It has been proven that $\Delta k_0 \in O(1/m)$, thus $m\Delta k_0$ is not dependent on m [1].

For an unbiased source, the product $\mathbf{A}^j\mathbf{s}_0^*$ is a zero vector by definition; however, in case of a biased source it contains non-zero elements. It can be expanded as a weighted sum of eigenvectors (keeping in mind $\mathbf{A}\mathbf{s}_0 = \mathbf{0}$)

$$\mathbf{A}^j\mathbf{s}_0^* = \mathbf{0} + a_1 \left(\frac{k_1}{k_0}\right)^j \mathbf{s}_1 + a_2 \left(\frac{k_2}{k_0}\right)^j \mathbf{s}_2 + \ldots \approx a_1 \left(\frac{k_1}{k_0}\right)^j \mathbf{s}_1 \tag{5.10}$$

where a-s are coefficients not dependent on m. From this the norm of the power series is approximated as

$$\left\| \sum_{j=1}^{\infty} \mathbf{A}^j \mathbf{s}_0^* \right\| \leq \sum_{j=1}^{\infty} \left\| \mathbf{A}^j \mathbf{s}_0^* \right\| \approx |a_1| \frac{k_1}{k_0} \left(1 - \frac{k_1}{k_0} \right)^{-1} \|\mathbf{s}_1\| \tag{5.11}$$

which shows that the sum converges to a value of the order $O(1)$ in m and the bias component $\bar{\boldsymbol{\varepsilon}}_B \in O(1/m)$.

Now the bound on the scalar relative error introduced by the bias can be written as

$$\bar{\varepsilon}_B \leq \frac{1}{m} B \tag{5.12}$$

where B is a constant dependent both on the system and the chosen norm type.

The $\bar{\varepsilon}_R$ component in Eq. (5.5) is the statistical error resulting from sampling of a finite number of histories. As was discussed earlier, this error is of the order $O(1/\sqrt{mn})$, and like for the component describing the bias, the bound of this component can similary be written as

$$\bar{\varepsilon}_R \leq \frac{1}{\sqrt{mn}} R \tag{5.13}$$

where R is another system and norm dependent constant.

To proceed, Eq. (3.28), the error propagation equation, is simplified into

$$\mathbf{e}^{(i)} = \mathbf{A}\mathbf{e}^{(i-1)} + O\left(m^{-1}\right) + \boldsymbol{\epsilon}^{(i-1)} \tag{5.14}$$

to overcome its non-linearity. Despite the simplification, The equation accounts for both the decrease of the error coming from the initial fission source and presence of the source bias.

This equation can be re-written as

$$\mathbf{e}^{(i)} = \mathbf{A}^i \mathbf{e}^{(0)} + O\left(m^{-1}\right) + \sum_{j=1}^{i} \mathbf{A}^{i-j} \boldsymbol{\epsilon}^{(j-1)} \tag{5.15}$$

yielding a decomposed relative error vector

$$\boldsymbol{\varepsilon}^{(i)} = \mathbf{A}^i \boldsymbol{\varepsilon}^{(0)} + \boldsymbol{\varepsilon}_B^{(i)} + \boldsymbol{\varepsilon}_R^{(i)} \tag{5.16}$$

Next, the initial fission source error vector is denoted as $\boldsymbol{\varepsilon}_0 = \boldsymbol{\varepsilon}^{(0)}$. From the previous it follows that

$$\boldsymbol{\varepsilon}_A^{(i)} = \mathbf{A}^i \boldsymbol{\varepsilon}_0 \tag{5.17}$$

According to properties of norms, this component of the scalar relative error is bounded by

$$\varepsilon_A^{(i)} = \|\mathbf{A}^i \boldsymbol{\varepsilon}_0\| \leq \|\mathbf{A}^i\| \|\boldsymbol{\varepsilon}_0\| = \varepsilon_0 \|\mathbf{A}^i\| \tag{5.18}$$

Since the noise propagation operator is a square matrix, it is known that

$$\lim_{j\to\infty} \|\mathbf{A}^j\|^{1/j} = \rho(\mathbf{A}) = \left|\frac{k_1}{k_0}\right| \tag{5.19}$$

where ρ stands for spectral radius. From this an approximation is obtained that improves quickly, cycle by cycle

$$\|\mathbf{A}^j\| \approx \left(\frac{k_1}{k_0}\right)^j \tag{5.20}$$

Finally, a bound for the $\varepsilon_A^{(i)}$ term in Eq. (5.4) is obtained as

$$\varepsilon_A^{(i)} \leq \varepsilon_0 \|\mathbf{A}^i\| \cong \varepsilon_0 \left(\frac{k_1}{k_0}\right)^i \tag{5.21}$$

which results in

$$\bar{\varepsilon}_A = \left\langle \varepsilon_A^{(n)} \right\rangle \leq \frac{1}{n}\sum_{i=1}^{n} \left(\frac{k_1}{k_0}\right)^i \varepsilon_0 \tag{5.22}$$

The scalar ε_0 is the relative error committed by guessing the initial fission source. This quantity is also norm dependent like the constants B and R.

From Eqs. (5.5), (5.12), (5.13), and (5.22) a bound for the scalar relative error in the cumulative fission source is obtained as

$$\bar{\varepsilon} \leq \frac{1}{n}\sum_{i=1}^{n} \left(\frac{k_1}{k_0}\right)^i \varepsilon_0 + \frac{B}{m} + \frac{R}{\sqrt{mn}} \tag{5.23}$$

This equation should be taken as a strong simplification, since the whole system is described solely by the dominance ratio. Nevertheless, finding a simple model was the authors' intention. Considering the availability of methods for on-the-fly dominance ratio estimation [19, 32], the model is certainly applicable.

5.2 STORM for batch size optimisation

In the following, a methodology is described for Monte Carlo ciritcality calculations with optimised values of neutron batch size. The method is dubbed STORM—the Stochastic rapidly convergent criticality method.

Firstly, the total number of simulated neutron histories h and the neutron batch size m are chosen to be the independent parameters, so that the total number of cycles n becomes

$$n = \frac{h}{m} \tag{5.24}$$

Based on the bound derived in Eq. (5.23), the equation used to model the changes in errors is written as

$$\hat{\varepsilon} = \frac{m\varepsilon_0}{h} \sum_{i=1}^{h/m} \left(\frac{k_1}{k_0}\right)^i + \frac{B}{m} + \frac{R}{\sqrt{h}} \tag{5.25}$$

For larger values of n, this equation can be further simplified by treating the finite sum as infinite, so that

$$\hat{\varepsilon} = \frac{m\varepsilon_0}{h} \left(1 - \frac{k_1}{k_0}\right)^{-1} + \frac{B}{m} + \frac{R}{\sqrt{h}} \tag{5.26}$$

which is a good approximation for the intended application of this equation, where the value of n will be relatively large.

The efficiency of the calculation is described by the figure of merit, which is defined as

$$\text{FOM} = \frac{1}{\hat{\varepsilon}^2 h} \tag{5.27}$$

where the standard deviation has been replaced with the relative error in the cumulative source and the computational time assumed proportional to the number of histories.

The figure of merit can be maximised by minimising the denominator in the equation above. The optimum condition is then written as

$$\frac{\partial(\hat{\varepsilon}^2 h)}{\partial m} = 2h\hat{\varepsilon} \left[\frac{\varepsilon_0}{h} \left(1 - \frac{k_1}{k_0}\right)^{-1} - \frac{B}{m^2}\right] = 0 \tag{5.28}$$

This equation can be rearranged into an expression for the neutron batch size

$$m = \sqrt{h \frac{B}{\varepsilon_0} \left(1 - \frac{k_1}{k_0}\right)} \tag{5.29}$$

which satisfies the optimum condition. The division in the term B/ε_0 compensates for scaling introduced by taking the norm of an error vector. The constant B describes how a certain system is affected by source biasing and is not calculable in general. It can be expected that the maximum relative error caused by the bias is one when a single neutron history is simulated per cycle; thus, for practical applications a simplification is made and B is assumed equal to one to obtain an equation for the optimal neutron batch size.

$$m_{opt} = \sqrt{\frac{h}{\varepsilon_0} \left(1 - \frac{k_1}{k_0}\right)} \tag{5.30}$$

given the total number of simulated neutron histories, dominance ratio of the system, and relative error in the initial fission source. This equation enables one to determine a value for the neutron batch size that balances its effects on the speed of source convergence and biasing of results.

In order to apply Eq. (5.30), the dominance ratio and the error in the initial fission source are needed. Fortunately, both quantities can be estimated with reasonable accuracy and effort during the initial stage of the Monte Carlo criticality calculation. Here it is suggested to evaluate these parameters during the simulation of a small fraction f (e.g. 1%) of the specified total number of neutron histories.

The dominance ratio can be evaluated by a number of methods, such as the NPM method [32], the CMFD based method [19], the CMPM [25] or even from the fission matrix. The error in the initial fission source can be estimated by the eigenvector of the fission matrix as

$$\tilde{\varepsilon}_0 = \frac{\|\mathbf{s}^{(0)}/m_0 - \mathbf{q}\|_1}{2} \tag{5.31}$$

where $\mathbf{s}^{(0)}$ is the initial fission source, m_0 is the neutron batch size chosen for the first n_0 cycles, and $\mathbf{q}$ is the eigenvector calculated from the fission matrix that was sampled during the initial cycles (normalised to one). If the fission matrix is not available, a very rough approximation can, instead, be taken as

$$\tilde{\varepsilon}_0 \cong \frac{\|\mathbf{s}^{(0)} - \mathbf{s}_c/n_0\|_1}{2m_0} \tag{5.32}$$

where $\mathbf{s}_c$ is the cumulative fission source combined over n_0 cycles. The factor 2 in Eqs. (5.31) and (5.32) scales the maximum possible value of $\tilde{\varepsilon}_0$ to one.

The estimation of dominance ratio is improved by simulating more cycles [24]; and since the bias is of no concern in these initial cycles, it is recommended to set a small value for m_0, for example so that $n_0 = m_0^2$. This results in $m_0 = \sqrt[3]{h_0}$, where h_0 is the number of histories used in the estimation stage. This will also ensure that the cumulative fission source is sufficiently different from the initial source to estimate its error if Eq. (5.32) is used.

Additionally, the sufficiency of the number of cycles can be assessed after an estimate is obtained, with a criterion adopted from [24]

$$(k_1/k_0)^n \leq \delta \tag{5.33}$$

where δ is a specified tolerance. This was suggested for the Coarse Mesh Projection method, but can be expected to be suitable for other noise propagation matrix based methods as well.

If the CMFD based method is used, it is advised to actually run the CMFD cycles of OpenMC [29] as the few last cycles (e.g. 10 or $m_0/2$) of the first stage. Since the batch size is very low, the CMFD solver makes the calculation of these cycles rather

slow; what is more, it is necessary for the calculation to have already converged to some extent to obtain accurate estimates of the dominance ratio.

After the initial stage, the estimated values of $\tilde{\varepsilon}_0$ and the dominance ratio are used in Eq. (5.30) to evaluate the optimal neutron batch size that is then used in the following cycles. An exemplary implementation is offered in Algorithm 1.

Algorithm 1 Conceptual implementation of STORM

input: h, f, $\mathbf{s}^{(0)}$
$m_0 \leftarrow \lceil \sqrt[3]{fh} \rceil$
$n_0 \leftarrow m_0^2$
$\mathbf{s}_c \leftarrow \mathbf{0}$
$i \leftarrow 1$
while $i \leq n_0$ **do** ▷ Initial cycles
    $\mathbf{s}^{(i)} \leftarrow$ Run MC cycle
    $\mathbf{s}_c \leftarrow \mathbf{s}_c + \mathbf{s}^{(i)}$
    $i \leftarrow i + 1$
end while
$k_1/k_0 \leftarrow$ Estimate dominance ratio
$\tilde{\varepsilon}_0 \leftarrow \|\mathbf{s}_c/n_0 - \mathbf{s}^{(0)}\|_1/2m_0$
$m \leftarrow \lceil \sqrt{h(1 - k_1/k_0)/\tilde{\varepsilon}_0} \rceil$
$n \leftarrow \lceil h/m \rceil$
while $i \leq n$ **do** ▷ Main cycles
    Run MC cycle
    $i \leftarrow i + 1$
end while

5.3 Test calculations

5.3.1 Numerical test model

Numerical test calculations were performed on a model of a common PWR fuel pin cell with parameters specified in Table 5.1. Reflective boundary conditions were applied on radial faces and void boundary conditions on axial faces. This model shares some features of a large core, e.g. a large dominance ratio.

Table 5.1: Specifications of the pin cell model.

Fuel	UO_2
Cladding material	Zr
Moderator	light water
Radius of fuel pellets	0.41 cm
Outer radius of cladding	0.475 cm
Rod pitch	1.26 cm
Length of the fuel rod	400 cm
^{235}U enrichment	3.1 wt%
Fuel density	10 g/cm^3
Moderator (water) density	0.7 g/cm^3

All numerical calculations were performed by an in-house non-analogue continuous-energy 3D Monte Carlo criticality code using the JEFF3.1 point-wise neutron cross-section library.

5.3.2 Reference calculation

The correct fission source distribution for the test system is not known and is estimated by a reference calculation specified in Table 5.2. As the test model is symmetrical, the source distribution $\mathbf{s}_r$ combined over the active cycles has been additionally symmetrised. The dominance ratio was estimated at 0.989 during the reference calculation by the NPM method [32] with a 10 cell axial mesh.

Table 5.2: Specifications of the reference calculation.

Number of histories per cycle	50,000
Number of active cycles	1,000,000
Number of inactive cycles	10,000
Initial fission source	flat

The reference solution is used in evaluating the error in the cumulative fission source in the test calculations. The scalar error in the cumulative fission source is

computed as

$$\varepsilon_c = \frac{\|\mathbf{s}_c/h - \mathbf{s}_r/h_r\|_1}{2} \tag{5.34}$$

where $\mathbf{s}_c$ and $\mathbf{s}_r$ are the fission sources combined over the cycles of test and reference calculations, respectively, and h_r is the total number of neutron histories simulated in the reference calculation. The factor in the denominator of Eq. (5.34) ensures the maximal possible value of ε_c to be one.

It should be noted that while the simplified model of the scalar error in the cumulative fission source captures the dependence of the error on the neutron batch size and other parameters, its direct comparison to the error computed by Eq. (5.34) is not trivial. This is not a problem for the presented optimisation methodology; it is merely an inconvenience when comparing the simplified model to results from test calculations, as the values do not necessarily have to match.

5.3.3 Demonstration of the simplified error model

The purpose of the calculations presented in this section is to demonstrate the usability of the simplified model of the scalar error in the cumulative fission source, given by Eq. (5.25). In this test, the simplified model is supplied with the dominance ratio estimated by the reference calculation; the constants B and R are assumed equal to one.

Four calculations, A–D, specified in Table 5.3, were repeated 40 times with various seeds for the random number generator. All calculations were started with a point source placed at one end of the pin, ensuring a large error in the initial fission source. Thus, the model assumes the maximum value $\varepsilon_0 = 1$.

Table 5.3: Specifications of calculations A–D.

Test calculation	A	B	C	D
Neutron histories per cycle	50	500	5000	50,000
Total number of histories		100 million		

In Fig. 5.1, the scalar errors in calculations A–D, computed by Eq. (5.34), are compared to the simplified model, given by Eq. (5.25). The results demonstrate that the simplified model correctly captures the dependence of the error on the neutron batch size and the total number of simulated neutron histories.

Fig. 5.1 also shows that performance of the calculation (given here by the error in the cumulative fission source) depends strongly on the neutron batch size; for a specific allocated computing cost (in terms of the total number of simulated neutron histories) the calculation performs best with a specific neutron batch size. For instance, when 10^7 neutron histories are to be simulated, the results achieved by simulating 500 neutron histories per cycle are significantly better than with other chosen values.

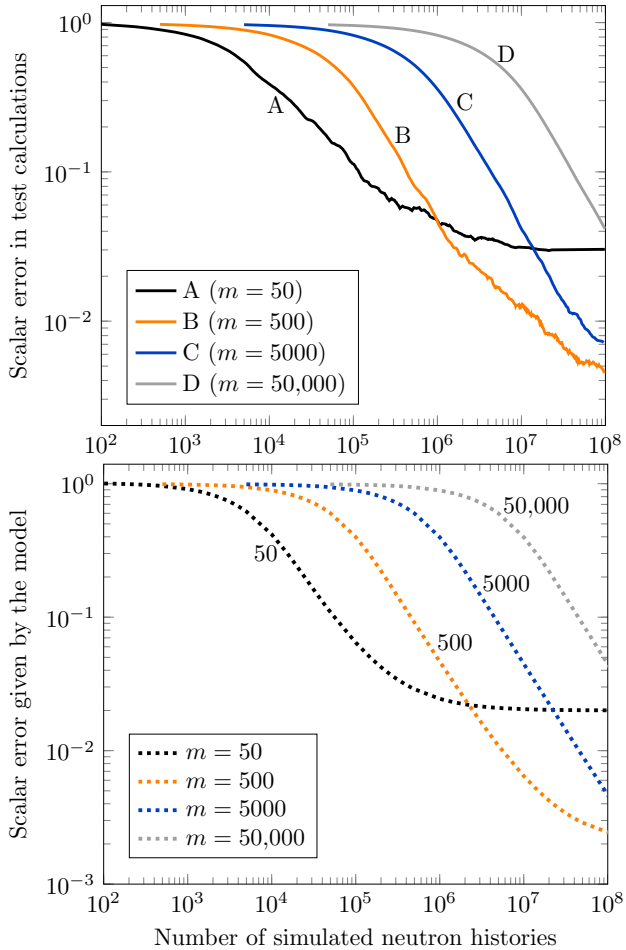

Figure 5.1: Top: scalar errors in calculations A–D computed by Eq. (5.34). Bottom: Scalar errors predicted by the simplified model, as in Eq. (5.25) for $m = 50$, 500, 5000 and 50,000.

5.3.4 Performance of calculations with optimal neutron batch size

Point source as initial fission source

In this section, the performance of Monte Carlo criticality calculations with the optimal neutron batch size estimated by Eq. (5.30) are demonstrated. In order to separate the effects of simplifications made in deriving Eq. (5.30) from the effects of errors present in the estimated parameters in Eq. (5.30), the dominance

ratio computed by the reference calculation is used. Such an accurate estimate of the dominance ratio would not be available in standard calculations; therefore, Sec. 5.3.5 includes numerical tests where the dominance ratio is computed in the beginning of the calculation, using a relatively small number of neutron histories, as suggested in Sec. 5.2.

Table 5.4: Specifications of calculations E–G.

Test calculation	E	F	G
Total number of histories	10^8	10^7	10^6
Optimal neutron batch size	1050	333	105

Table 5.4 shows the optimal neutron batch size calculated by Eq. (5.30) for three values of allocated computing cost (10^8, 10^7 and 10^6 simulated neutron histories); the three cases are marked as E, F, and G. For this, the dominance ratio was set to 0.989, and the relative error in the initial fission source was set to the maximum value $\varepsilon_0 = 1$ (the same initial source was used as in Sec. 5.3.3).

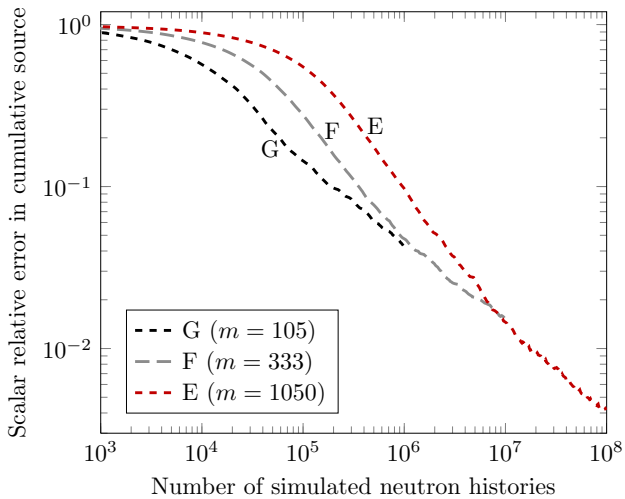

Figure 5.2: Results of calculations E–G. Neutron batch size optimisation is compared in calculations of different length.

Monte Carlo criticality calculations for cases E, F, and G were repeated 40 times with different seeds, and the resulting errors were averaged. Fig. 5.2 compares the performance of these cases, and demonstrates the effectiveness of the optimal neutron batch size computed by Eq. (5.30) for various cases. For instance, when 10^6 neutron histories were simulated, the calculation with the neutron batch size optimised for 10^6 neutron histories (case G) performed better than the calculation with

the neutron batch size optimised for 10^8 neutron histories (case E). Nevertheless, we can see that case F (optimised for 10^7 neutron histories) performed similarly to case G when 10^6 neutron histories were simulated, which suggests that the optimal value of the neutron batch size does not necessarily have to be computed very accurately in order to achieve good performance. This simplifies the application of the methodology since the input parameters, such as the dominance ratio or the error in the initial fission source, may be estimated less accurately in the beginning of the calculation.

In this section, case E (with the neutron batch size optimised for 10^8 histories) is also compared to two additional calculations where the neutron batch size was set to suboptimal values of 10,000 (case H) and 100 (case I). Calculations H and I were also repeated 40 times and averaged. Fig. 5.3 shows that calculation E (optimal) achieved orders of magnitude smaller errors than calculations H and I after simulating 10^8 neutron histories.

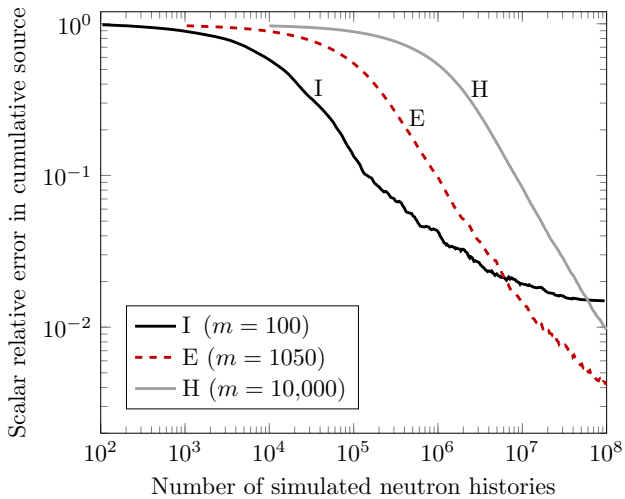

Figure 5.3: Results of test calculations E, H, and I. Results given by the optimal neutron batch size (1050) are compared to results obtained by using unoptimised parameters.

Flat source as initial fission source

All test calculations presented so far used point sources as initial fission source guesses to ensure large initial errors. This choice was made in favour of a more effective presentation of results and does not mean the methodology is limited to such cases. The proposed batch size optimisation is equally effective when flat initial sources are used.

An additional test case, J, was specified to test the batch size optimisation with flat initial sources. It is compared to test case E, thus, the total number of histories was taken as 10^8 and calculations were repeated 40 times. Reference dominance ratio was assumed and the error in the initial source was assumed to be $\varepsilon_0 = 0.2$. This resulted in the optimal value of 2 350 for the batch size.

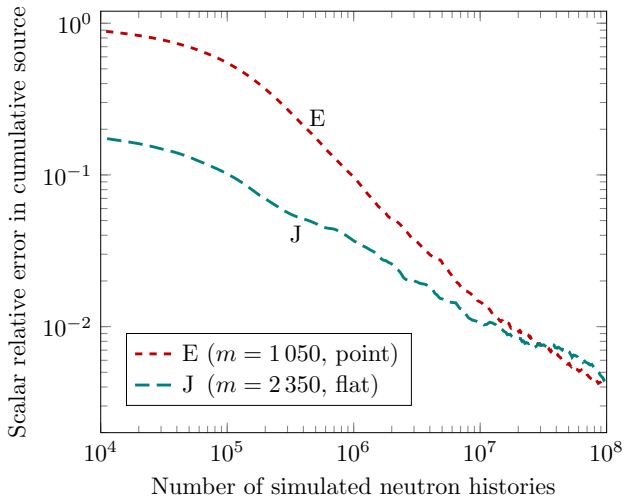

Figure 5.4: Results of calculations E and J. Neutron batch size optimisation is compared in calculations with different initial fission sources.

Fig. 5.4 presents results from test calculations E and J, where different initial sources were compared. It can be seen that a better initial source guess causes the errors to be smaller in the beginning of the calculation. However, after simulating all of the neutron histories, the erroros caused by the point source have decayed to an equally low value. No other batch size was found to produce smaller errors.

5.3.5 Demonstration of STORM

The purpose of this section is to test the neutron batch size optimisation methodology for Monte Carlo criticality calculations, or STORM, as suggested in Sec. 5.2, assuming no knowledge of the correct dominance ratio or the error in the initial fission source. Therefore, as suggested in Sec. 5.2, the calculation is split into two stages; the dominance ratio and the error in the initial fission source are estimated in the short first stage, while the neutron batch size is corrected to the optimal value for the second stage.

The total allocated computational cost was set to 10^8 neutron histories for this test. As suggested in Sec. 5.2, 1% of the computing cost (10^6 neutron histories)

was allocated to the first stage of the calculation. According to suggestions in Sec. 5.2, the neutron batch size for the first stage was set to $\sqrt[3]{10^6} = 100$.

During the first STORM stage, the dominance ratio was estimated at 0.9876 by the NPM method; in order to keep the method general and not optimised for a specific test model, a $3 \times 3 \times 3$ spatial mesh was used. The error in the initial fission source was estimated at 0.9941. Based on these values, the optimal neutron batch size was evaluated at 1120, and the batch size was changed to this value for the second stage of the calculation. The value of the dominance ratio estimated during the first step of this calculation does not differ much from the value computed during the reference calculation; hence, the optimal value of the neutron batch size calculated here (1120) does not differ much from the test case E (1050).

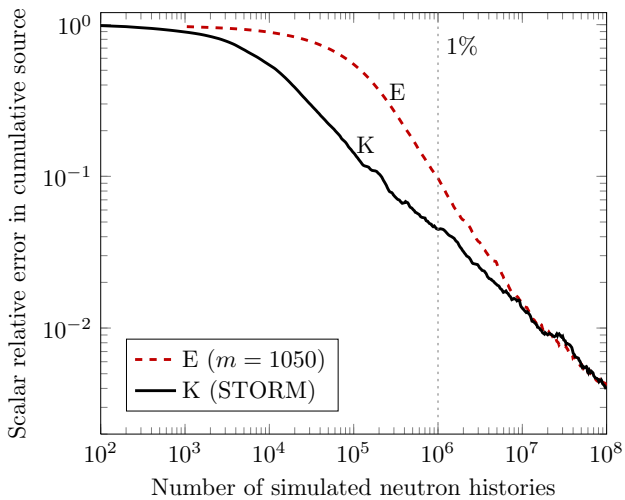

Figure 5.5: Results of calculations by STORM (K) and optimised by reference parameters (E).

The two-stage STORM calculation was repeated 40 times, and results were averaged, as in all previous calculations. Fig. 5.5 compares the performance of the STORM calculation (marked as case K) to the test case E (that used the neutron batch size optimised for 10^8 neutron histories). As can be seen, both calculations perform equally well when 10^8 neutron histories are simulated. Naturally, the two-stage STORM calculation converged faster during the first stage, as the neutron batch size was forced to be small; however, this did not change the final results.

5.4 Conclusions

In this chapter, a simplified equation was derived to model the scalar relative error in the cumulative source. The model relates the error to the chosen total number of neutron histories, neutron batch size, dominance ratio of the system, and error in the initial fission source. Numerical test calculations showed that even though the equation is strongly simplified, it describes the changes sufficiently well, providing information that enables the optimisation of neutron batch size.

From the simplified error model, an equation was derived to determine an optimal neutron batch size which maximises the efficiency of calculations. This is achieved by balancing the effects of source convergence speed and biasing of results. In order to apply this result, a methodology was suggested for neutron batch size optimisation. Subsequent test calculations demonstrated that the calculated optimal batch size ensures the best possible results and that the methodology is usable in practical applications. The method is general in nature and implementable in any power method based Monte Carlo code that comes equipped with a dominance ratio estimation procedure.

It should be noted that the optimal neutron batch size may also be affected by the use of parallelised calculations; for example, the master-slave parallel-computing scheme performs better with a larger neutron batch size. However, the derived optimisation methodology does not consider the efficiency of various parallel-computing schemes and differences in computer architectures.

Chapter 6

Summary

The thesis at hand concentrates on Monte Carlo criticality calculations—a method of solving the steady-state homogeneous k-eigenvalue neutron transport equation. The introductory part of the text introduces the mentioned equation and discusses what it is commonly used for. Following that, solving the transport equation by the stochastic sampling (Monte Carlo) method is explained to the extent necessary for understanding the presented work.

The main objective of the presented research was to improve the efficiency of Monte Carlo criticality calculations. It is known that the choice of the number of neutron histories that are simulated in each cycle of the calculation (the neutron batch size) affects the overall efficiency. On one hand, a small neutron batch size allows the calculation to converge faster from the guessed initial fission source to a stationary source distribution; on the other hand, a systematic error, inversely proportional to the batch size, is always present in the results.

In this work, it is suggested that the general calculation error can be characterised by the error in the cumulative fission source, i.e. the fission source combined over all simulated cycles. This choice was made because Monte Carlo calculations combine the results of all cycles to estimate quantities of interest and errors in the fission source can affect all other possible results. The work establishes that these errors describe both the decrease of errors introduced by the starting fission source and the fission source bias. Additionally, if this error is combined with the allocated computational time (in terms of the total number of simulated neutron histories) the efficiency of the calculation can be described.

Existing theory about source convergence and error propagation in Monte Carlo criticality calculations is summarised and a mathematical notation is adopted for further analysis of errors. A mathematical treatment of the relative error in the cumulative fission source is given.

Following that, a method for direct estimation of errors in the cumulative Monte Carlo fission source is suggested. The method proposes to utilise two qualities of the

fission matrix. Firstly, it is known that the fission matrix can be sampled correctly even if the fission source contains a large bias, as long as the spatial mesh cells are sufficiently small. Secondly, it has been observed that the eigenvector of the fission matrix (which is equivalent to the fission source distribution) converges faster than the cumulative fission source. The proposed method suggests to use the eigenvector of the fission matrix to estimate errors in the cumulative fission source. Results of numerical test calculations support the efficacy of the method.

The fission matrix eigenvector method gives important results in error estimation of Monte Carlo criticality calculations. The traditional variance estimates fail to capture errors caused by systematic biases and errors caused by the starting fission source that remain in the results. The suggested error estimation method allows one to estimate the order of magnitude of real errors, including those caused by the two aforementioned phenomena. This is important for the credibility of results, since all calculated values, including the power distribution or the multiplication factor, are affected by errors in the fission source distribution.

Undoubtedly, the method has its shortcomings. As it was said, the mesh used for sampling the fission matrix has to be sufficiently fine; however, it is not known how to determine this sufficiency in the general case. This is a topic that needs further study for any fission matrix based method to be applied. Sec. 3.4 may offer possible ideas for this problem. What is more, the fission matrix eigenvector method for error estimation needs further testing in calculations to confirm its validity and to verify if its results are distributed normally around real errors.

The described direct estimation of errors does not provide analytic information that would allow for any optimisation. For this reason, a simplified model is derived to describe the relative error in the cumulative fission source. This model relates the error to the chosen neutron batch size, the total number of simulated neutron histories, the dominance ratio of the system, and the relative error in the initial fission source. The model is tested by numerical calculations and shown to be sufficient for describing the changes in errors over the simulated cycles.

The simplified error model is further applied in finding an expression for the optimal value of the neutron batch size for certain allocated computing time (in the form of the total number of simulated neutron histories). An equation is derived giving the optimal batch size as a function of the total number of simulated neutron histories, the dominance ratio, and the error in the initial source. The optimum condition is verified by numerical test calculations.

As the dominance ratio and the error in the initial source are unknown in general, a new method is proposed, dubbed STORM—the Stochastic rapidly convergent criticality method. The developed methodology suggests a two-stage calculation, where the first stage uses a small fraction of the total number of neutron histories to estimate the dominance ratio and the error in the initial source; these estimates are then used to set the optimal neutron batch size for the second stage to ensure maximum efficiency of the calculation. The method is tested and proven in practical

applications by numerical test calculations.

First of all, the analysis demonstrates that the choice of neutron batch size has significant effects on the performance of calculations. As the neutron batch size is commonly not optimised, the calculations either reach biased solutions or they converge slowly and errors originating from the initial source remain in results. The developed methodology ensures that for a certain allocated computational time, the best possible results are obtained, thanks to the optimal choice of neutron batch size. This is an important result for longer, computationally more expensive simulations.

The formulation of STORM has its shortcomings, too. The error model is strongly simplified and may perform worse than expected in some cases. What is more, in deriving the optimal neutron batch size, an additional simplification was made in one constant, which may require further study and improvement. The correct implementation of STORM is dependent on the appropriate setup of the initial stage and the dominance ratio estimation method to be used, which will require some testing.

Both methods developed in this work, the fission matrix eigenvector method for error estimation and STORM, are rather general in nature and implementable in any power method based Monte Carlo criticality code. The fission matrix eigenvector method requires the fission matrix to be sampled, and STORM is applicable with any dominance ratio estimation method. Both required features are available in a variety of existing codes, making it possible to apply the developed methods in practical applications.

The thesis met its objective in developing a method that improves the efficiency of Monte Carlo criticality calculations. Neutron batch size optimisation and STORM have great potential in improving the effectiveness of the computational time spent on Monte Carlo calculations; and the fission matrix eigenvector error estimation method allows the monitoring of real calculation errors. It is the hope of the author that both methods would be studied further and considered for implementation in Monte Carlo criticality codes.

Bibliography

[1] Brissenden, R. J., and Garlick, A. R. Biases in the estimation of k_{eff} and its error by Monte Carlo methods. *Annals of Nuclear Energy 13*, 2 (1986), 63–83.

[2] Brown, F. A review of best practices for Monte Carlo criticality calculations. Tech. Rep. LA-UR-09-03136, Los Alamos National Laboratory, 2009.

[3] Brown, F., Carney, S., Kiedrowski, B., and Martin, W. Fission matrix capability for MCNP, part I – theory. Tech. Rep. LA-UR-13-20429, Los Alamos National Laboratory, 2013.

[4] Carter, L. L., and Cashwell, E. D. *Particle-transport simulation with the Monte Carlo method.* Energy Research and Development Administration, 1975.

[5] Carter, L. L., and McCormick, N. J. Source convergence in Monte Carlo calculations. *Nuclear Science and Engineering 36* (1969), 438–441.

[6] Dubi, A., and Elperin, T. On the markov chain analysis of source iteration Monte Carlo procedures for criticality problems: II. *Nuclear Science and Engineering 91*, 1 (1985), 77–83.

[7] Duderstadt, J. J., and Martin, W. R. *Transport Theory.* Wiley-Interscience, 1979.

[8] Dufek, J. *Development of new Monte Carlo methods in Reactor Physics.* PhD thesis, KTH Royal Institue of Technology, Stockholm, 2009.

[9] Dufek, J., and Gudowski, W. Fission matrix based Monte Carlo criticality calculations. *Annals of Nuclear Energy 36*, 8 (2009), 1270–1275.

[10] Dufek, J., and Gudowski, W. Stability and convergence problems of the Monte Carlo fission matrix acceleration methods. *Annals of Nuclear Energy 36*, 10 (2009), 1648–1651.

[11] Enosh, M., Shalitin, D., and Yeivin, Y. The bias in Monte Carlo eigenvalue calculations. *Progress in Nuclear Energy 24* (1990), 259–269.

[12] Forster, R. A., Little, R. C., Briesmeister, J. F., and Hendricks, J. S. MCNP capabilities for nuclear well logging calculations. *IEEE Transactions on Nuclear Science 37*, 3 (1990), 1378.

[13] Gast, R. C. Monte Carlo eigenfunction iteration strategies that are and are not fair games. Tech. Rep. WAPD-TM-878, 1969.

[14] Gast, R. C., and Candelore, N. R. Monte Carlo eigenfunction strategies and uncertainties. In *Proceedings of NEACRP Meeting of a Monte Carlo Study Group* (Argonne National Laboratory, 1974).

[15] Gelbard, E. M. Biases in Monte Carlo eigenvalue calculations. In *IMACS-International Symposium on Scientific Computing and Mathematical Modeling* (Bangalore, India, 1992).

[16] Gelbard, E. M., and Gu, A. G. Biases in Monte Carlo eigenvalue calculations. *Nuclear Science and Engineering 117* (1994), 1–9.

[17] Gelbard, E. M., and Prael, R. Computation of standard deviations in eigenvalue calculations. *Progress in Nuclear Energy 24*, 1–3 (1990), 237–241. Monte Carlo Methods for Neutrons and Photon Transport Calculations.

[18] Gelbard, E. M., and Prael, R. E. Monte Carlo work at Argonne National Laboratory. In *Proceedings of NEACEP Monte Carlo Specialists Meeting* (Argonne National Laboratory, July 1974).

[19] Herman, B. R., Forget, B., and Smith, K. Utilizing CMFD in OpenMC to estimate dominance ratio and adjoint. In *Transactions of the American Nuclear Society* (Washington, D.C., November 2013), vol. 109.

[20] Kalos, M. H., and Whitlock, P. A. *Monte Carlo Methods*. WILEY-VCH Verlag GmbH & Co., 2008.

[21] Los Alamos National Laboratory, X-5 Monte Carlo Team. *MCNP — A General Monte Carlo N-Particle Transport Code, Version 5 Volume I: Overview and Theory*, February 2008.

[22] MacMillan, D. B. Monte Carlo confidence limits for iterated-source calculations. *Nuclear Science and Engineering 50* (1973), 73–75.

[23] Nease, B. R. *Time series analysis of Monte Carlo neutron transport calculations*. PhD thesis, University of New Mexico, 2008.

[24] Nease, B. R., Brown, F. B., and Ueki, T. Dominance ratio calculations with MCNP. In *Proc. Int. Topical Mtg. on Physics of Reactors* (Sept 2008).

[25] Nease, B. R., and Ueki, T. Time series analysis of Monte Carlo fission sources—III: coarse-mesh projection. *Nuclear Science and Engineering 157* (2007), 51–64.

[26] Nease, B. R., and Ueki, T. Time series analysis and Monte Carlo methods for eigenvalue separation in neutron multiplication problems. *Journal of Computational Physics 228* (2009), 8525–8547.

[27] TRIPOLI-4.4 Monte Carlo Method Particle Transport Code, NEA-1716, 2008. Abstract available from: http://www.nea.fr/abs/html/nea-1716.html.

[28] Richtmyer, R. D., and von Neumann, J. Statistical methods in neutron diffusion. Tech. Rep. LAMS-551, Los Alamos National Laboratory, 1947.

[29] Romano, P. K., and Forget, B. The OpenMC Monte Carlo particle transport code. *Annals of Nuclear Energy 51* (2013), 274–281.

[30] SCALE: A Modular Code System for Performing Standardized Computer Analyses for Licensing Evaluation, ORNL/TM-2005/39, Version 5.1, Vols. I–III, 2006. Available from Radiation Safety Information Computational Center at Oak Ridge National Laboratory as CCC-732.

[31] Shim, H. J., and Kim, C. H. Real variance estimation using an intercycle fission source correlation for Monte Carlo eigenvalue calculations. *Nuclear Science and Engineering 162* (2009), 98–108.

[32] Sutton, T. M., Romano, P. K., and Nease, B. R. On-the-fly Monte Carlo Dominance Ratio calculation using the Noise Propagation Matrix. *Progress in Nuclear Science and Technology 2* (2011), 749–756.

[33] Ueki, T. Intergenerational correlation in Monte Carlo k-eigenvalue calculation. *Nuclear Science and Engineering 141* (2002), 101–110.

[34] Ueki, T., Brown, F. B., Parsons, D. K., and Kornreich, D. E. Autocorrelation and dominance ratio in Monte Carlo criticality calculations. *Nuclear Science and Engineering 145* (2003), 279–290.

[35] Ueki, T., Brown, F. B., Parsons, D. K., and Warsa, J. S. Time series analysis of Monte Carlo fission sources—I: Dominance Ratio computation. *Nuclear Science and Engineering 148* (2004), 374–390.

[36] Ueki, T., Mori, T., and Nakagawa, M. Error estimations and their biases in monte carlo eigenvalue calculations. *Nuclear Science and Engineering 125*, 1 (1997), 1–11.

[37] Wikipedia. Neutron transport — wikipedia, the free encyclopedia, 2014. [Online; accessed 21-May-2014].

[38] Zolotukhin, V. G., and Maiorov, L. V. An estimate of the systematic errors in the calculations of criticality by the Monte Carlo method. *Atomnaya Energia 55*, 3 (1983), 173.

Estimation of errors in the cumulative Monte Carlo fission source

Kaur Tuttelberg[a,*], Jan Dufek[a]

[a] *KTH Royal Institute of Technology, Division of Nuclear Reactor Technology*
AlbaNova University Center, 10691 Stockholm, Sweden

Abstract

We study the feasibility of estimating the error in the cumulative fission source in Monte Carlo criticality calculations by utilising the fundamental-mode eigenvector of the fission matrix. The cumulative fission source, representing the source combined over active cycles, contains errors of both statistical and systematic nature. Knowledge of the error in the cumulative fission source is crucial as it determines the accuracy of computed neutron flux and power distributions.

While statistical errors are present in the eigenvector of the fission matrix, it appears that these are not (or they are only weakly) correlated to the errors in the cumulative fission source. This ensures the suggested methodology gives error estimates that are distributed around the real errors, which is also supported by results of our numerical test calculations.

Keywords: Monte Carlo, criticality, fission source, cumulative, convergence, error, bias

1. Introduction

Conventional Monte Carlo criticality calculations simulate subsequent neutron generations in so-called cycles. The fission source is expected to converge to the steady-state during a certain number of inactive cycles in which no results are being collected. Results of interest are then combined over a number of active cycles. While the fission source is supposed to be converged during the active cycles, there is no diagnostics methodology that could guarantee that with certainty, although progress has been made in this field (Ueki and Brown, 2003). Hence, the fission source may be sampled during the active cycles from a distribution that is far from steady-state; moreover, the fission source may also contain a bias not decaying over the cycles at all (Brissenden and Garlick, 1986). Consequently, the fission source introduces errors into the results sampled over the active cycles (such as the neutron flux and power distributions). We could accept this fact if we had the knowledge of the error in the cumulative fission source (i.e., the error in the fission source that was combined over the active cycles).

The purpose of this paper is to investigate the feasibility of estimating the error in the cumulative fission source. The estimate should reflect not only the error due to the convergence problems; it should also reflect the bias and random errors. We investigate the possibility of achieving this goal via utilising the fundamental-mode eigenvector of the fission matrix. The fission matrix has been already used in a number of unrelated methods (Carter and McCormick, 1969; Kadotani et al., 1991; Kitada and Takeda, 2001; Dufek and Gudowski, 2009; Brown et al., 2013a,b), and a number of established Monte Carlo criticality codes offer the fission matrix as an optional result. Naturally, the fission matrix contains random errors that are also present in its eigenvector; in this paper, we analyse whether these errors allow using the eigenvector for estimating the error in the cumulative fission source.

The paper is organised as follows. Aspects of convergence of the Monte Carlo fission source are briefly described in Section 2. The methodology of estimating the error in the cumulative fission source is suggested in Section 3. Results of the numerical test calculations are given in Section 4. Our conclusions are summarised in Section 5.

2. Aspects of source convergence

The eigenvalue (criticality) equation for the fission source can be written as

$$ks(\mathbf{r}) = Hs(\mathbf{r}), \tag{1}$$

where k is the eigenvalue, $s(\mathbf{r})$ is the concentration of fission neutrons at $\mathbf{r}$, and

$$Hs(\mathbf{r}) \equiv \int_V \mathrm{d}^3 r'\, f(\mathbf{r}' \to \mathbf{r}) s(\mathbf{r}'),$$

where $f(\mathbf{r}' \to \mathbf{r})\,\mathrm{d}^3 r$ is an expected number of first generation fission neutrons produced in the volume element $\mathrm{d}^3 r$ at $\mathbf{r}$, resulting from a fission neutron born at $\mathbf{r}'$. Angular dependence is not considered since fission neutrons are emitted isotropically. The Monte Carlo fission source is represented by a batch of m neutrons with specific positions, energies, and statistical weights.

*Corresponding author.
Email address: kaurt@kth.se (Kaur Tuttelberg)

Eq. (1) has many eigen-pair solutions, s_j and k_j, but only the fundamental-mode solution (corresponding to the largest eigenvalue) has a physical meaning. The respective modes are commonly ordered according to the absolute value of their eigenvalue, from the largest (associated with the fundamental mode $j = 0$) to the smallest. To simplify the notation in the following text, we denote the fundamental-mode fission source as z; $z \equiv s_0$.

To obtain the fundamental-mode solution, Monte Carlo criticality codes apply the power iteration on the fission source; this iteration can be formally described as

$$s^{(i+1)} = \frac{1}{k^{(i)}} H s^{(i)} + \epsilon^{(i)} \tag{2}$$

$$k^{(i)} = \frac{\int_V \mathrm{d}^3 r \, H s(\mathbf{r})}{m} \tag{3}$$

where the steps $i = 0, 1, \ldots$ are commonly referred to as "cycles", $\epsilon^{(i)}(\mathbf{r})$ is the random error component resulting from sampling a finite number of neutron histories in cycle i. The initial fission source $s^{(0)}$ must be guessed. The above iteration assumes that the Monte Carlo fission source is always normalised to m; i.e.,

$$\int_V \mathrm{d}^3 r \, s(\mathbf{r}) = m.$$

In classical Monte Carlo criticality calculations, a number of inactive cycles must be performed just to decay the error present in $s^{(0)}$, while results of interest are sampled over the subsequent active cycles.

As with any Monte Carlo simulation, the random error component $\epsilon^{(i)}(\mathbf{r})$ is of the order $O(1/\sqrt{m})$. Moreover, we can assume that (Gelbard and Gu, 1994)

$$\mathrm{E}[\epsilon^{(i)}] = 0.$$

The random noise in the fission source can thus be reduced by simulating more neutron histories, at the expense of a larger computing time. The random noise in the fission source $\epsilon^{(i)}$ is, however, not a relevant problem as long as the results are combined over a sufficiently large number of active cycles n. The random noise in the cumulative fission source

$$s_{\mathrm{c}}^{(n)} = \sum_{i=i_{\mathrm{x}}+1}^{n} s^{(i)}, \tag{4}$$

being of the order $O(1/\sqrt{mn})$, can then be neglected. In Eq. (4), i_{x} denotes the number of inactive cycles.

Gelbard and Prael (1974) showed that the random errors propagate over the cycles of Monte Carlo criticality calculations, which results in the presence of a bias in the fission source of the order $O(1/m)$. Thus, the converged Monte Carlo fission source is never sampled from the correct fundamental mode z, but from a biased fundamental mode that we denote as z_m. This bias is indeed reflected in the cumulative fission source. We show an example of a biased cumulative fission source in Section 4.

Ueki et al. (2003) have shown that convergence of the Monte Carlo fission source $s^{(i)}$ to z_m is governed by the dominance ratio k_1/k_0 at the rate of $O((k_1/k_0)^i)$. This is also a well known fact in deterministic calculations (although the solution is not biased there). This has an important consequence to systems with dominance ratio close to unity; if the initial fission source contains a large error then many cycles are necessary to decay this error. There is a risk then that active cycles (and hence the cumulative fission source) will be corrupted.

3. Estimating the error in the cumulative Monte Carlo fission source

In discrete phase-space notation, the eigenvalue (criticality) equation for the fission source can be written as

$$\mathbf{H}\mathbf{s} = k\mathbf{s} \tag{5}$$

where $\mathbf{H}$ is commonly referred to as the fission matrix (Carter and McCormick, 1969). The fission matrix $\mathbf{H}$ is the space-discretised operator H; The $(i,j)^{\mathrm{th}}$ element of $\mathbf{H}$ represents the probability that a fission neutron born in space zone j causes a subsequent birth of a fission neutron in space zone i,

$$\mathbf{H}[i,j] = \frac{\int_{\mathrm{Z}_i} \mathrm{d}^3 r \int_{\mathrm{Z}_j} \mathrm{d}^3 r' f(\mathbf{r}' \to \mathbf{r}) z(\mathbf{r}')}{\int_{\mathrm{Z}_j} \mathrm{d}^3 r' \, z(\mathbf{r}', E')}. \tag{6}$$

The fundamental mode eigenvalue of $\mathbf{H}$ equals k_{eff}, and the corresponding eigenvector $\mathbf{h}$ equals the discretised fundamental mode fission source $z(\mathbf{r})$.

A number of Monte Carlo codes, e.g. TRIPOLI-4 (OECD/NEA, 2008) and KENO V.a (RSICC, 2006), can optionally calculate the fission matrix during standard Monte Carlo calculations. Dufek and Gudowski (2009) showed that the fission matrix becomes less sensitive to errors in the fission source as the mesh zones get smaller. Hence, the errors in the fission source become irrelevant for sampling the fission matrix when the zones are sufficiently small. This means that the fission matrix and its fundamental-mode eigenvector can be correctly evaluated during a Monte Carlo criticality calculation even with a biased fission source. We suggest utilising this quality of the eigenvector of the fission matrix in estimating the error in the cumulative fission source.

We define the relative scalar error ε in the cumulative fission source $\mathbf{s}_{\mathrm{c}}^{(n)}$ discretised over a space mesh as

$$\varepsilon = \left\| \tilde{\mathbf{s}}_{\mathrm{c}}^{(n)} - \tilde{\mathbf{z}} \right\|_1, \tag{7}$$

where $\sim$ denotes a normalisation operator defined for any vector $\mathbf{x}$ as

$$\tilde{\mathbf{x}} = \frac{\mathbf{x}}{\|\mathbf{x}\|_1}.$$

and the one-norm is defined as

$$\|\mathbf{x}\|_1 = \sum_i |x_i|.$$

In Eq. (7), $\mathbf{z}$ is the fundamental-mode source discretised over the same mesh as the cumulative fission source.

The fundamental-mode source $\mathbf{z}$ in Eq. (7) is unknown; hence, the correct value of ε cannot be computed. We suggest to estimate its value as

$$\hat{\varepsilon} = \left\| \tilde{\mathbf{s}}_{\mathrm{c}}^{(n)} - \tilde{\mathbf{h}}^{(n)} \right\|_1, \tag{8}$$

where $\mathbf{h}^{(n)}$ is the eigenvector of the fission matrix $\mathbf{H}^{(n)}$ that was sampled over the same cycles as the cumulative fission source $\mathbf{s}_{\mathrm{c}}^{(n)}$.

Naturally, the fission matrix $\mathbf{H}^{(n)}$ contains random errors of the order $O(1/\sqrt{nm})$ that must also be present in its eigenvector $\mathbf{h}^{(n)}$. We denote the random errors in $\tilde{\mathbf{h}}^{(n)}$ by the vector $\boldsymbol{\delta}^{(n)}$,

$$\boldsymbol{\delta}^{(n)} = \tilde{\mathbf{h}}^{(n)} - \tilde{\mathbf{z}}; \tag{9}$$

while we denote the errors in $\tilde{\mathbf{s}}_{\mathrm{c}}^{(n)}$ by the vector $\boldsymbol{\gamma}^{(n)}$,

$$\boldsymbol{\gamma}^{(n)} = \tilde{\mathbf{s}}_{\mathrm{c}}^{(n)} - \tilde{\mathbf{z}},$$

so that

$$\varepsilon = \sum_i \left| \gamma_i^{(n)} \right|.$$

Then we can write Eq. (8) as

$$\hat{\varepsilon} = \left\| \boldsymbol{\gamma}^{(n)} - \boldsymbol{\delta}^{(n)} \right\|_1, \tag{10}$$

that can also be written as

$$\hat{\varepsilon} = \sum_i \left| \gamma_i^{(n)} - \delta_i^{(n)} \right|, \tag{11}$$

Note that $\boldsymbol{\gamma}^{(n)}$ contains not only statistical errors, but also the bias and the partly decayed errors coming from the initial fission source.

Since both $\tilde{\mathbf{h}}^{(n)}$ and $\tilde{\mathbf{z}}$ are normalised to unity, we can write

$$\sum_i \left| \tilde{h}_i^{(n)} \right| = \sum_i |\tilde{z}_i|, \tag{12}$$

Since all elements in $\tilde{\mathbf{h}}^{(n)}$ and $\tilde{\mathbf{z}}$ are non-negative, the absolute value signs can be removed,

$$\sum_i \left(\tilde{h}_i^{(n)} - \tilde{z}_i \right) = 0, \tag{13}$$

which is equivalent to

$$\sum_i \delta_i^{(n)} = 0. \tag{14}$$

Hence, the vector $\boldsymbol{\delta}^{(n)}$ must contain both positive and negative elements so that their sum would equal zero. This quality of $\boldsymbol{\delta}^{(n)}$ suggests that the expected value of $\hat{\varepsilon}$ equals

$$\mathrm{E}(\hat{\varepsilon}) = \sum_i \left| \gamma_i^{(n)} \right| = \varepsilon, \tag{15}$$

assuming that $\boldsymbol{\delta}^{(n)}$ and $\boldsymbol{\gamma}^{(n)}$ are not correlated. Hence, if this condition is satisfied then the error estimate $\hat{\varepsilon}$ given by Eq. (8) is normally distributed around ε. It is, however, not apparent whether this condition is satisfied. The purpose in the numerical calculations in Section 4 is to analyse this.

4. Numerical test calculations

4.1. Numerical test model

The numerical test model represents a fuel pin cell with parameters summarised in Table 1. Reflective boundary conditions were applied to all radial faces; non-reflective void boundary conditions were applied to the axial faces. This model is based on a common PWR fuel pin cell; only the pin length was increased to 10 m in order to achieve the dominance ratio of a large core.

Table 1: Specifications of the pin cell model.

Fuel	UO_2
Cladding material	Zr
Moderator	light water
Radius of fuel pellets	0.41 cm
Outer radius of cladding	0.475 cm
Rod pitch	1.26 cm
Length of the fuel rod	1000 cm
^{235}U enrichment	3.1 wt%
Fuel density	10 g/cm^3
Moderator (water) density	0.7 g/cm^3

Based on the fission matrix computed during the reference calculation (see Sec. 4.2), we have evaluated the dominance ratio of the test model at 0.9982, which ensures that convergence of the fission source is similar to that in large reactor cores and loosely-coupled systems.

All numerical calculations were performed by an in-house non-analogue continuous-energy 3D Monte Carlo criticality code using the JEFF3.1 point-wise neutron cross-section library.

4.2. Reference calculation

The fundamental-mode of the fission source is not available in an analytical form for the numerical test model; hence the need for a reference calculation. Parameters of the reference calculation are summarised in Table 2. The reference distribution of the fission source, $\mathbf{s}_{\mathrm{ref}}$, was evaluated via a sufficiently fine uniform mesh with 100 axial zones, and combined over all active cycles. As the test

model is axially symmetrical, we have further improved the accuracy of $\mathbf{s}_{\text{ref}}$ by averaging its elements in symmetrical positions.

Table 2: Parameters of the reference calculation.

Neutron batch size	50,000
Number of active cycles	2,000,000
Number of inactive cycles	2000
Initial fission source	flat

Fig. 1 depicts the reference solution together with an example of a biased cumulative fission source obtained via a criticality calculation with a batch size of only 10 neutrons. While the bias in the reference solution is negligible (due to the large neutron batch size), the biased fission source shows the typical flattening of its distribution.

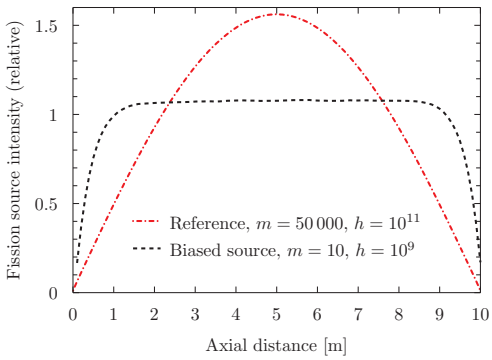

Figure 1: The reference fission source and an example of a biased fission source (b denotes the neutron batch size, and h denotes the total number of neutron histories simulated in active cycles).

4.3. Estimating the error in the cumulative source

Table 3 specifies the test calculations (A-D). While the neutron batch size varied in calculations A-D, all calculations simulated 10^9 neutron histories. The initial fission source was randomly sampled from a uniform distribution in the first cycle of each calculation. In each calculation, the fission matrix was sampled over all cycles; no cycles were skipped.

Table 3: Parameters of calculations A-D.

Calculation	A	B	C	D
Neutron batch size	50	500	5000	50,000
Number of neut. hist.	10^9	10^9	10^9	10^9

For the purpose of the test calculations, we set the axial dimension of all zones to 10 cm; hence, we evaluate the fission matrix via a spatial mesh with 100 zones. This mesh appears sufficient for eliminating the bias in the fission

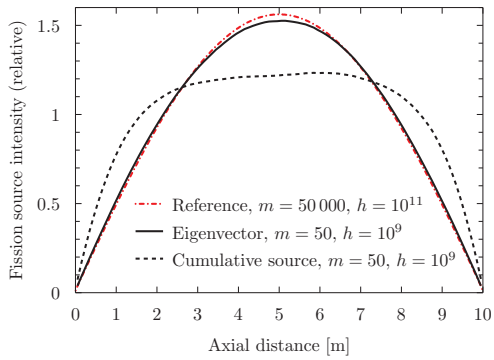

Figure 2: Comparison of the reference solution and the eigenvector of a fission matrix sampled by a biased fission source.

matrix (that could possibly arise from the biased fission source). This is demonstrated in Fig. 2 that compares the eigenvector of the fission matrix to the cumulative fission source biased by the batch size of 50 neutrons; the fission matrix was sampled by the actual biased fission source. While the fission source is heavily biased, the eigenvector of the fission matrix is close to the reference solution in Fig. 2.

In calculations A-D, the real relative error ε in the cumulative fission source distribution $\mathbf{s}_{\text{c}}$ is evaluated as

$$\varepsilon = \left\| \tilde{\mathbf{s}}_{\text{c}} - \tilde{\mathbf{s}}_{\text{ref}} \right\|_1 . \tag{16}$$

The estimation $\hat{\varepsilon}$ of the relative error in a cumulative fission source is computed according to Eq. (8).

The values of $\hat{\varepsilon}$ and ε obtained from all the test cases are compared in Tables 4-7. In each calculation, the values of $\hat{\varepsilon}$ and ε are calculated at several stages, always after simulating 10^6, 10^7, 10^8 and 10^9 neutron histories. To associate a certain value of $\hat{\varepsilon}$ or ε to a certain stage, we add a superscript in square brackets to $\hat{\varepsilon}$ and ε, denoting the number of simulated neutron histories; e.g., the values of $\hat{\varepsilon}^{[10^9]}$ and $\varepsilon^{[10^9]}$ are computed after simulating 10^9 neutron histories.

Results from calculation A (with the batch size of 50 neutrons) are summarised in Table 4. As the bias in the fission source is large due to the small neutron batch size (as depicted in Fig. 1), $\varepsilon^{[10^7]}$, $\varepsilon^{[10^8]}$ and $\varepsilon^{[10^9]}$ remain about equally large, close to 20%. This is correctly captured by the corresponding values of $\hat{\varepsilon}^{[10^7]}$, $\hat{\varepsilon}^{[10^8]}$ and $\hat{\varepsilon}^{[10^9]}$. The value of $\hat{\varepsilon}^{[10^6]}$ is less than half of that of $\varepsilon^{[10^6]}$; in this case, the relatively large random errors in the eigenvector of fission matrix (that was sampled by only 10^6 neutron histories) decreased the estimated error.

Results from calculation B (with the batch size of 500 neutrons) are summarised in Table 5. Here, values of $\hat{\varepsilon}$ also correspond well to ε, with the exception of the value of $\hat{\varepsilon}^{[10^8]}$ that underestimated the real error several times.

Results from calculation C (with the batch size of 5000 neutrons) are summarised in Table 6. This case shows

Table 4: Comparison of ε and $\hat{\varepsilon}$ in calculation A (with the batch size of **50** neutrons) [%].

h (# of neutron histories)	$\varepsilon^{[h]}$	$\hat{\varepsilon}^{[h]}$
10^6	36.7	14.9
10^7	18.3	18.4
10^8	18.1	18.2
10^9	20.2	18.6

Table 5: Comparison of ε and $\hat{\varepsilon}$ in calculation B (with the batch size of **500** neutrons) [%].

h (# of neutron histories)	$\varepsilon^{[h]}$	$\hat{\varepsilon}^{[h]}$
10^6	24.0	19.8
10^7	12.4	8.21
10^8	3.78	1.10
10^9	4.53	3.63

that $\hat{\varepsilon}$ may overestimate the real error several times as well; note the value of $\hat{\varepsilon}^{[10^6]}$ and $\hat{\varepsilon}^{[10^7]}$. The small bias in the cumulative fission source combined over 10^9 neutron histories was correctly estimated.

Table 6: Comparison of ε and $\hat{\varepsilon}$ in calculation C (with the batch size of **5000** neutrons) [%].

h (# of neutron histories)	$\varepsilon^{[h]}$	$\hat{\varepsilon}^{[h]}$
10^6	17.7	41.0
10^7	8.23	18.3
10^8	8.41	6.44
10^9	1.17	1.25

Results from calculation D (with the batch size of 50,000 neutrons) are summarised in Table 7. In this case, $\hat{\varepsilon}$ estimated the real error in the cumulative fission source in all stages of the calculation with a good accuracy.

We wish to stress that the above results depend on the initial seed value in the RNG; as such, $\hat{\varepsilon}$ is a random variable. Repeating the identical calculation with another seed would produce different results (both $\hat{\varepsilon}$ and ε). Nevertheless, the above results suggest clearly that $\hat{\varepsilon}$ can be used in estimating the order of magnitude of the error in the cumulative fission source.

5. Conclusions

The fact that the fission matrix can be well sampled even by a biased or not converged Monte Carlo fission source can be utilised for various purposes. In this paper, we have analysed the possibility of using the fundamental-mode eigenvector of the fission matrix for estimating the error in the cumulative fission source. The question we attempted to answer was whether the random errors, that are naturally present in the eigenvector, allow us to obtain a useful estimation of the error in the cumulative fission source.

Table 7: Comparison of ε and $\hat{\varepsilon}$ in calculation D (with the batch size of **50,000** neutrons) [%].

h (# of neutron histories)	$\varepsilon^{[h]}$	$\hat{\varepsilon}^{[h]}$
10^6	37.9	28.2
10^7	26.1	25.1
10^8	4.51	4.29
10^9	1.15	1.25

We can conclude that the estimation of the error in the cumulative fission source obtained via the eigenvector of the fission matrix is distributed around the real error, assuming that the random errors in the eigenvector and the cumulative fission source are not correlated. Validity of this assumption is, however, not apparent. Nevertheless, our numerical test calculations confirmed the error estimates were distributed around the real errors, which suggests the errors are either not correlated or the correlation is weak. The error estimations correctly captured the presence of the source bias as well as the source errors coming from the initial fission source.

The future research may consider testing of the suggested methodology using better statistics on a variety of systems, including radially heterogeneous, full-core systems. Further attention may also be devoted to analysing the impact of the space mesh quality on the results.

Acknowledgements

This work was partly funded by the European Commission under the High Performance Monte Carlo Reactor Core Analysis (HPMC) project, within the 7$^{\text{th}}$ EU Framework Program, Project Number 295971.

This research was also supported by Estonian scholarship program Kristjan Jaak, which is funded and managed by Archimedes Foundation in collaboration with the Ministry of Education and Research.

References

Brissenden, R. J., Garlick, A. R., 1986. Biases in the estimation of k_{eff} and its error by Monte Carlo methods. Ann. Nucl. Energy 13 (2), 63–83.

Brown, F., Carney, S., Kiedrowski, B., Martin, W., October 27–31 2013. Fission matrix capability for MCNP Monte Carlo. In: Joint International Conference on Supercomputing in Nuclear Applications + Monte Carlo (SNA + MC 2013).

Brown, F., Carney, S., Kiedrowski, B., Martin, W., May 2013. Fission matrix capability for MCNP, Part I - Theory. In: Proc. ANS Topical Meeting M&C2013, International Conference on Mathematics and Computational Methods Applied to Nuclear Science and Engineering, Sun Valley, Idaho.

Carter, L. L., McCormick, N. J., 1969. Source convergence in Monte Carlo calculations. Nucl. Sci. Eng. 36, 438–441.

Dufek, J., Gudowski, W., 2009. Fission matrix based Monte Carlo criticality calculations. Ann. Nucl. Energy 36 (8), 1270–1275.

Gelbard, E. M., Gu, A. G., 1994. Biases in Monte Carlo eigenvalue calculations. Nucl. Sci. Eng. 117, 1–9.

Gelbard, E. M., Prael, R. E., July 1974. Monte Carlo work at Argonne National Laboratory. In: Proceedings of NEACEP Monte Carlo Specialists Meeting. Argonne National Laboratory.

Kadotani, H., Hariyama, Y., Shiota, M., Takeda, T., September 9-13 1991. Acceleration of fission distribution convergence using eigenvectors from matrix k calculations in the KENO code. In: ICNC 91. Oxford, UK, paper II-1.

Kitada, T., Takeda, T., 2001. Effective convergence of fission source distribution in Monte Carlo simulation. J. Nucl. Sci. Technol. 38 (5), 324–329.

OECD/NEA Data Bank Computer Program Services, 2008. TRIPOLI-4.4 Monte Carlo Method Particle Transport Code, NEA-1716. Abstract available from: http://www.nea.fr/abs/html/nea-1716.html.

RSICC, 2006. SCALE: A Modular Code System for Performing Standardized Computer Analyses for Licensing Evaluation, ORNL/TM-2005/39, Version 5.1, Vols. IIII. Available from Radiation Safety Information Computational Center at Oak Ridge National Laboratory as CCC-732.

Ueki, T., Brown, F. B., April 6-11 2003. Stationarity and source convergence diagnostics in Monte Carlo criticality calculation. In: Nuclear Mathematical and Computational Sciences: A Century in Review, A Century Anew. Gatlinburg, Tennessee.

Ueki, T., Brown, F. B., Parsons, D. K., Kornreich, D. E., 2003. Autocorrelation and dominance ratio in Monte Carlo criticality calculations. Nucl. Sci. Eng. 145, 279–290.

Neutron batch size optimisation methodology for Monte Carlo criticality calculations

Kaur Tuttelberg[a,*], Jan Dufek[a]

[a] *KTH Royal Institute of Technology, Division of Nuclear Reactor Technology, AlbaNova University Center, 10691 Stockholm, Sweden*

Abstract

We present a methodology that improves the efficiency of conventional Monte Carlo criticality calculations by optimising the number of neutron histories simulated per criticality cycle (the so-called neutron batch size). The chosen neutron batch size affects both the rate of convergence (in computing time) and magnitude of bias in the fission source. Setting a small neutron batch size ensures a rapid simulation of criticality cycles, allowing the fission source to converge fast to its stationary state; however, at the same time, the small neutron batch size introduces a large systematic bias in the fission source. It follows that for a given allocated computing time, there is an optimal neutron batch size that balances these two effects.

We approach this problem by studying the error in the cumulative fission source, i.e. the fission source combined over all simulated cycles, as all results are commonly combined over the simulated cycles. We have derived a simplified formula for the error in the cumulative fission source, taking into account the neutron batch size, the dominance ratio of the system, the error in the initial fission source and the allocated computing time (in the form of the total number of simulated neutron histories). Knowing how the neutron batch size affects the error in the cumulative fission source allows us to find its optimal value. We demonstrate the benefits of the method on a number of numerical test calculations.

Keywords: Monte Carlo criticality, source convergence, source bias, error propagation, dominance ratio, optimisation

1. Introduction

Monte Carlo criticality calculations require the user to set a number of free parameters, namely the number of active and inactive cycles, neutron batch size, and the initial fission source. The efficiency of calculations is affected by the choice of these parameters, most of all by the neutron batch size. Generally, a large neutron batch size is preferred in order to decrease the systematic biases (Brown, 2009; Gast, 1969; Gast and Candelore, 1974). However, a large neutron batch size limits the number of cycles that can be simulated in allocated computational time, hence, the error originating from the initial fission source may not decrease sufficiently, corrupting the accumulated results. Thus, the selection of neutron batch size represents an optimisation problem.

The errors in the fission source, including the source bias and the error originating from the initial fission source, directly affect all possible results of Monte Carlo criticality calculations that are collected over a number of cycles. Hence, for the purpose of this paper, we find it reasonable to define the general error of the calculation, that we need in evaluating the computing efficiency (the figure of merit), as the error in the cumulative fission source.

In this paper, we present a simplified model for the error in the cumulative fission source. The model estimates the error based on the neutron batch size, the chosen total number of neutron histories to be simulated, the dominance ratio of the system, and the estimated error in the initial fission source. Using this model, we can determine the optimal neutron batch size to achieve the maximum figure of merit.

The existing source convergence theory is summarised in Sec. 2 and the simplified error model is derived in Sec. 3. Following that, the optimal batch size is derived in Sec. 4. Sec. 5 contains the description and results of numerical test calculations. Our conclusions are presented in Sec. 6.

2. Governing equations

Monte Carlo criticality calculations solve the steady-state k-eigenvalue neutron transport equation. This equation, in operator notation, can be written as

$$\mathbf{H}\mathbf{s}_j = k_j \mathbf{s}_j \tag{1}$$

where k_j and $\mathbf{s}_j$ constitute the eigenpairs of $\mathbf{H}$, an operator comprising the terms of an angle and energy integrated transport equation.

Eq. (1) presents an eigenvalue equation translated into discretised phase-space (Gelbard, 1992; Gelbard and Gu, 1994; Gelbard and Prael, 1974). In this notation, the system is divided into spatial regions. Such a notation is only adopted to simplify the mathematical framework needed to carry out the theoretical analysis.

*Corresponding author
Email address: kaurt@kth.se (Kaur Tuttelberg)

As a part of this discretisation, the operator in the eigenvalue equation is described as a matrix, known as the fission matrix (Brown et al., 2013; Carter and McCormick, 1969). In a similar manner, the fission source distribution is represented as a vector where each element specifies the number of fission neutrons in the corresponding discrete space cell.

In the laid out notation, a cycle in the eigenvalue calculation can be described as (Gelbard and Prael, 1974)

$$\mathbf{s}^{(i+1)} = \frac{\mathbf{H}\mathbf{s}^{(i)}}{k^{(i)}} + \boldsymbol{\epsilon}^{(i)} \tag{2}$$

where $\mathbf{s}^{(i)}$ and $\mathbf{s}^{(i+1)}$ are fission source vectors in consecutive cycles and $\boldsymbol{\epsilon}^{(i)}$ is the stochastic error component resulting from sampling a finite number of histories per cycle. The eigenvalue, $k^{(i)}$, is estimated as an integral quantity of the fission source

$$k^{(i)} = \frac{\boldsymbol{\tau}\mathbf{H}\mathbf{s}^{(i)}}{m} \tag{3}$$

where m is the number of neutrons sampled in the cycle—the neutron batch size—and the vector $\boldsymbol{\tau} = (1, 1, \ldots, 1)$ is an integral operator in the same dimension as the number of discretisation cells. A normalisation is imposed on the fission source in each cycle, ensuring that $\boldsymbol{\tau}\mathbf{s}^{(i)} = m$.

Estimates for quantities of interest are averaged over the cycles. For any quantity x the mean, or ensemble average, $\langle x^{(n)} \rangle$ over n cycles is defined as

$$\left\langle x^{(n)} \right\rangle = \frac{1}{n} \sum_{i=1}^{n} x^{(i)} \tag{4}$$

where $x^{(i)}$ is the i^{th} cycle estimate of x.

Eq. (2) presents an iterative process, very much like the power method. Eigenvalue powering converges to the fundamental mode eigenpair; and in this light, it is common to order the eigenvalues descendingly by the modulus, starting from the highest ($k_0 > |k_1| > \ldots$). The convergence of the power method is governed by the ratio k_1/k_0—the dominance ratio (Goult et al., 1975). It has been reasoned that the dominance ratio also characterises the convergence of Monte Carlo criticality calculations (Ueki et al., 2003, 2004).

As it is characteristic for Monte Carlo calculations, the errors of statistical sampling in combined results are of the order $O(1/\sqrt{mn})$, with mn being the total number of neutron histories simulated over n cycles. These errors are always decreased by increasing the number of simulated histories and are not dependent on the choice of neutron batch size. For any Monte Carlo process it is assumed that $\mathrm{E}[\boldsymbol{\epsilon}^{(i)}] = 0$ (Gelbard and Prael, 1974).

It has been long known that the results of Monte Carlo eigenvalue calculations contain systematic errors. The magnitude of these errors, known as biases, have been shown to be inversely proportional to the neutron batch size (Brissenden and Garlick, 1986; Dubi and Elperin, 1985; Enosh et al., 1990; Zolotukhin and Maiorov, 1983). By definition, the bias in the Monte Carlo estimate of the fundamental mode eigenvector is (Gelbard and Prael, 1974)

$$\Delta\mathbf{s}_0 = \mathbf{s}_0^* - \mathbf{s}_0 = \left\langle \frac{1}{m}\mathbf{s}^{(n)} \right\rangle - \mathbf{s}_0 \tag{5}$$

where $\mathbf{s}_0$ is the correct fundamental mode eigenvector of Eq. (1) and $\mathbf{s}_0^*$ is the biased estimate, both normalised to unity. The definition of bias is based on the assumption that the calculation has converged and the statistical errors have become negligible. Following suit, the eigenvalue bias is defined as

$$\Delta k_0 = k_0^* - k_0 = \left\langle k^{(n)} \right\rangle - k_0 \tag{6}$$

where asterisk denotes a biased quantity, like above.

Brissenden and Garlick (1986) have shown how to quantify the bias in the eigenvalue; however, calculating the bias in the fission source has remained an unsolved problem. Nevertheless, we can learn more about it by analysing cycle-wise error propagation.

The fission source error in cycle i is introduced as

$$\mathbf{e}^{(i)} = \mathbf{s}^{(i)} - m\,\mathbf{s}_0. \tag{7}$$

In order to analyse such error vectors, Eq. (7) is substituted into (2) and the latter expanded in series as

$$\begin{aligned}\mathbf{e}^{(i+1)} = &\sum_{j=0}^{\infty} \left(-\frac{\boldsymbol{\tau}\mathbf{H}\mathbf{e}^{(i)}}{k_0 m \boldsymbol{\tau}\mathbf{s}_0} \right)^j \left[\frac{\mathbf{H}\left(m\,\mathbf{s}_0 + \mathbf{e}^{(i)}\right)}{k_0 \boldsymbol{\tau}\mathbf{s}_0} \right] \\ &- m\,\mathbf{s}_0 + \boldsymbol{\epsilon}^{(i)}.\end{aligned} \tag{8}$$

As the biases are of the order $O(1/m)$, the terms of a smaller order in m can be disregarded (Brissenden and Garlick, 1986; Gelbard and Prael, 1974). After normalising the fundamental mode eigenvector to unity, $\boldsymbol{\tau}\mathbf{s}_0 = 1$, Eq. (8) can be simplified to

$$\mathbf{e}^{(i+1)} \cong \mathbf{A}\mathbf{e}^{(i)} - \frac{\boldsymbol{\tau}\mathbf{H}}{k_0 m}\mathbf{e}^{(i)}\mathbf{A}\mathbf{e}^{(i)} + \boldsymbol{\epsilon}^{(i)}. \tag{9}$$

The operator $\mathbf{A}$—the noise propagation matrix—in Eq. (9) is a result of combining terms in the expansion of the error vector,

$$\mathbf{A} = \frac{\mathbf{I} - \mathbf{s}_0\boldsymbol{\tau}}{k_0}\mathbf{H} \tag{10}$$

where $\mathbf{I}$ is the identity matrix (Gelbard and Prael, 1974). It has been shown that the highest modulus eigenvalue of the noise propagation matrix corresponds to the dominance ratio of the system (Nease, 2008; Nease and Ueki, 2009).

Gelbard (1992) showed that after a large enough number of cycles, when the process is stationary, noted by $\langle \mathbf{e}^{(n)} \rangle \cong \langle \mathbf{e}^{(n-1)} \rangle$, Eq. (9) yields

$$\left\langle \mathbf{e}^{(n)} \right\rangle = -\frac{(\mathbf{I} - \mathbf{A})^{-1}}{k_0 m}\mathbf{A}\left\langle \mathbf{e}^{(n)}\mathbf{e}^{(n)\mathsf{T}} \right\rangle \mathbf{H}^{\mathsf{T}}\boldsymbol{\tau}^{\mathsf{T}}. \tag{11}$$

This shows that the iteration converges to a non-zero value—the bias.

In addition to the error vector specified in Eq. (7), we define the relative error in one cycle as the error normalised to one neutron history

$$\boldsymbol{\varepsilon}^{(i)} = \frac{\mathbf{e}^{(i)}}{m} = \frac{\mathbf{s}^{(i)}}{m} - \mathbf{s}_0 \,. \tag{12}$$

For any relative error vector $\boldsymbol{\varepsilon}$, we define its magnitude as its norm

$$\varepsilon = \|\boldsymbol{\varepsilon}\|. \tag{13}$$

We define the error $\bar{\varepsilon}$ in the cumulative fission source (the source combined over all cycles) as the relative error $\boldsymbol{\varepsilon}^{(i)}$ averaged over n cycles,

$$\bar{\boldsymbol{\varepsilon}} = \left\langle \boldsymbol{\varepsilon}^{(n)} \right\rangle = \frac{1}{n}\sum_{i=1}^{n} \boldsymbol{\varepsilon}^{(i)} = \frac{1}{mn}\sum_{i=1}^{n} \mathbf{e}^{(i)}. \tag{14}$$

For a stationary process, the relative error in the cumulative fission source is equal to the bias $\Delta\mathbf{s}_0$; hence, the relative error decays into the bias in conditions matching its definition (i.e. no significant contribution from other sources of error). A method for direct estimation of the error in the cumulative fission source was proposed by Tuttelberg and Dufek (2014); however, such an approach does not provide analytical information needed for neutron batch size optimisation.

3. Simplified model of the error in the cumulative fission source

First of all, we choose to decompose the error vector into three components

$$\mathbf{e}^{(i)} = \mathbf{e}_A^{(i)} + \mathbf{e}_B^{(i)} + \mathbf{e}_R^{(i)} \tag{15}$$

where the first term, $\mathbf{e}_A^{(i)}$, describes the decay of the error coming from the initial fission source; the second term, $\mathbf{e}_B^{(i)}$, includes the bias; and the third term, $\mathbf{e}_R^{(i)}$, is the stochastic error component.

We express the scalar relative error in cycle i as

$$\varepsilon^{(i)} = \|\boldsymbol{\varepsilon}^{(i)}\| = \|\boldsymbol{\varepsilon}_A^{(i)} + \boldsymbol{\varepsilon}_B^{(i)} + \boldsymbol{\varepsilon}_R^{(i)}\|. \tag{16}$$

By properties of norms, the value on the right hand side has an upper bound of

$$\|\boldsymbol{\varepsilon}_A^{(i)} + \boldsymbol{\varepsilon}_B^{(i)} + \boldsymbol{\varepsilon}_R^{(i)}\| \leq \|\boldsymbol{\varepsilon}_A^{(i)}\| + \|\boldsymbol{\varepsilon}_B^{(i)}\| + \|\boldsymbol{\varepsilon}_R^{(i)}\| \tag{17}$$

so that

$$\varepsilon^{(i)} \leq \varepsilon_A^{(i)} + \varepsilon_B^{(i)} + \varepsilon_R^{(i)} \tag{18}$$

which implies

$$\bar{\varepsilon} \leq \bar{\varepsilon}_A + \bar{\varepsilon}_B + \bar{\varepsilon}_R \,. \tag{19}$$

We specified Eq. (15) so that the $\mathbf{e}_B^{(i)}$ component describes the bias; thus, when the calculation has become stationary, we can write

$$\bar{\boldsymbol{\varepsilon}}_B = \Delta\mathbf{s}_0 = \left\langle \frac{\mathbf{e}^{(n)}}{m} \right\rangle. \tag{20}$$

Based on that and Eq. (11), we can continue by writing

$$\bar{\boldsymbol{\varepsilon}}_B = -\frac{1}{m}\left(\mathbf{I} - \mathbf{A}\right)^{-1} \mathbf{A} \left\langle \frac{\mathbf{e}^{(n)}\mathbf{e}^{(n)\mathsf{T}}}{m} \right\rangle \frac{\mathbf{H}^{\mathsf{T}}\boldsymbol{\tau}^{\mathsf{T}}}{k_0} \,. \tag{21}$$

It is possible to show that this component is in fact of the order $O(1/m)$, as we would expect from the bias.

As the fundamental mode eigenvalue of the noise propagation matrix is equivalent to the dominance ratio of the system, we know that the spectral radius of the matrix is less than one, allowing us to write the inverse as a Neumann series

$$\left(\mathbf{I} - \mathbf{A}\right)^{-1} = \sum_{j=0}^{\infty} \mathbf{A}^j. \tag{22}$$

From the definition of cycle-wise error it follows that

$$\mathbf{A}\left\langle \frac{\mathbf{e}^{(n)}}{m} \right\rangle = \mathbf{A}\mathbf{s}_0^*$$

and

$$\left\langle \mathbf{e}^{(n)\mathsf{T}} \right\rangle \mathbf{H}^{\mathsf{T}}\boldsymbol{\tau}^{\mathsf{T}} = m\Delta k_0 \,.$$

The norm is then expressed as

$$\|\bar{\boldsymbol{\varepsilon}}_B\| \leq \left| -\frac{1}{m} \right| \left\| \sum_{j=1}^{\infty} \mathbf{A}^j \mathbf{s}_0^* \right\| \left| \frac{m\Delta k_0}{k_0} \right|. \tag{23}$$

Brissenden and Garlick (1986) proved that $\Delta k_0 \in O(1/m)$, thus $m\Delta k_0$ is not dependent on m.

For an unbiased source, the product $\mathbf{A}^j\mathbf{s}_0^*$ is a zero vector by definition; however, in case of a biased source it contains non-zero elements. We expand it as a weighted sum of eigenvectors (keeping in mind $\mathbf{A}\mathbf{s}_0 = \mathbf{0}$)

$$\begin{aligned} \mathbf{A}^j\mathbf{s}_0^* &= \mathbf{0} + a_1\left(\frac{k_1}{k_0}\right)^j \mathbf{s}_1 + a_2\left(\frac{k_2}{k_0}\right)^j \mathbf{s}_2 + \dots \\ &\approx a_1\left(\frac{k_1}{k_0}\right)^j \mathbf{s}_1 \end{aligned} \tag{24}$$

where a-s are coefficients not dependent on m. From this we approximate the norm of the power series as

$$\left\| \sum_{j=1}^{\infty} \mathbf{A}^j\mathbf{s}_0^* \right\| \leq \sum_{j=1}^{\infty} \left\| \mathbf{A}^j\mathbf{s}_0^* \right\| \approx |a_1| \frac{k_1}{k_0}\left(1 - \frac{k_1}{k_0}\right)^{-1} \|\mathbf{s}_1\| \tag{25}$$

which shows that the sum converges to a value of the order $O(1)$ in m; and the bias component $\bar{\boldsymbol{\varepsilon}}_B \in O(1/m)$.

Now we can write the bound on the scalar relative error introduced by the bias as

$$\bar{\varepsilon}_B \leq \frac{1}{m} B \tag{26}$$

where B is a constant dependent both on the system and the chosen norm type. Similarly, we write the bound for the $\bar{\varepsilon}_R$ component as

$$\bar{\varepsilon}_R \leq \frac{1}{\sqrt{mn}} R \tag{27}$$

where R is another system and norm dependent constant.

To proceed, we simplify Eq. (9), the error propagation equation, into

$$\mathbf{e}^{(i)} = \mathbf{A}\mathbf{e}^{(i-1)} + O\left(m^{-1}\right) + \boldsymbol{\epsilon}^{(i-1)} \tag{28}$$

to overcome its non-linearity. This equation can be rewritten as

$$\mathbf{e}^{(i)} = \mathbf{A}^i \mathbf{e}^{(0)} + O\left(m^{-1}\right) + \sum_{j=1}^{i} \mathbf{A}^{i-j} \boldsymbol{\epsilon}^{(j-1)} \tag{29}$$

yielding a decomposed relative error vector

$$\boldsymbol{\varepsilon}^{(i)} = \mathbf{A}^i \boldsymbol{\varepsilon}^{(0)} + \boldsymbol{\varepsilon}_B^{(i)} + \boldsymbol{\varepsilon}_R^{(i)} . \tag{30}$$

We denote $\boldsymbol{\varepsilon}_0 = \boldsymbol{\varepsilon}^{(0)}$ and write

$$\boldsymbol{\varepsilon}_A^{(i)} = \mathbf{A}^i \boldsymbol{\varepsilon}_0 . \tag{31}$$

According to properties of norms, this component of the scalar relative error is bounded by

$$\varepsilon_A^{(i)} = \|\mathbf{A}^i \boldsymbol{\varepsilon}_0\| \leq \|\mathbf{A}^i\| \|\boldsymbol{\varepsilon}_0\| = \varepsilon_0 \|\mathbf{A}^i\| . \tag{32}$$

Since the noise propagation operator is a square matrix, we know that

$$\lim_{j\to\infty} \|\mathbf{A}^j\|^{1/j} = \rho(\mathbf{A}) = \left|\frac{k_1}{k_0}\right| \tag{33}$$

where ρ stands for spectral radius. From this we obtain an approximation that improves quickly, cycle by cycle

$$\|\mathbf{A}^j\| \approx \left(\frac{k_1}{k_0}\right)^j . \tag{34}$$

Finally, we obtain a bound for the $\varepsilon_A^{(i)}$ term in Eq. (18) as

$$\varepsilon_A^{(i)} \leq \varepsilon_0 \|\mathbf{A}^i\| \cong \varepsilon_0 \left(\frac{k_1}{k_0}\right)^i \tag{35}$$

which results in

$$\bar{\varepsilon}_A = \left\langle \varepsilon_A^{(n)} \right\rangle \leq \frac{1}{n} \sum_{i=1}^{n} \left(\frac{k_1}{k_0}\right)^i \varepsilon_0 . \tag{36}$$

The scalar ε_0 is the relative error committed by guessing the initial fission source. This quantity is also norm dependent like the constants B and R.

From Eqs. (19), (26), (27), and (36) we obtain a bound for the scalar relative error in the cumulative fission source as

$$\bar{\varepsilon} \leq \frac{1}{n} \sum_{i=1}^{n} \left(\frac{k_1}{k_0}\right)^i \varepsilon_0 + \frac{B}{m} + \frac{R}{\sqrt{mn}} . \tag{37}$$

This equation is presented as a strong simplification, where the whole system is described solely by the dominance ratio. Nevertheless, finding a simple model was the authors' intention. Considering the availability of methods for on-the-fly dominance ratio estimation (Herman et al., 2013; Sutton et al., 2011), the model is certainly applicable.

4. Derivation of optimal neutron batch size

We choose the total number of simulated neutron histories h and neutron batch size m to be independent parameters; hence, the total number of cycles n is

$$n = \frac{h}{m} . \tag{38}$$

Based on the bound derived in Eq. (37), the equation we use to model the changes in errors is written as

$$\hat{\varepsilon} = \frac{m\varepsilon_0}{h} \sum_{i=1}^{h/m} \left(\frac{k_1}{k_0}\right)^i + \frac{B}{m} + \frac{R}{\sqrt{h}} . \tag{39}$$

For larger values of n, this equation can be further simplified by treating the finite sum as infinite, so that

$$\hat{\varepsilon} = \frac{m\varepsilon_0}{h} \left(1 - \frac{k_1}{k_0}\right)^{-1} + \frac{B}{m} + \frac{R}{\sqrt{h}} \tag{40}$$

which is a good approximation for the intended application of this equation, where the value of n will be relatively large.

The efficiency of the calculation is described by the figure of merit, which we will define as

$$\mathrm{FOM} = \frac{1}{\hat{\varepsilon}^2 h} \tag{41}$$

where we have replaced the standard deviation with the relative error in the cumulative source and assumed the computational time proportional to the number of histories.

The figure of merit can be maximised by minimising the denominator in the equation above. The optimum condition is then written as

$$\frac{\partial(\hat{\varepsilon}^2 h)}{\partial m} = 2h\hat{\varepsilon} \left[\frac{\varepsilon_0}{h} \left(1 - \frac{k_1}{k_0}\right)^{-1} - \frac{B}{m^2}\right] = 0 . \tag{42}$$

This equation can be rearranged into an expression for the neutron batch size

$$m = \sqrt{h \frac{B}{\varepsilon_0} \left(1 - \frac{k_1}{k_0}\right)} \tag{43}$$

which satisfies the optimum condition. The division in the term B/ε_0 compensates for scaling introduced by taking the norm of an error vector. The constant B describes how a certain system is affected by source biasing and is not calculable in general. We can expect that the maximum relative error caused by the bias is one when a single neutron history is simulated per cycle; thus, for practical applications we make a simplification and assume $B = 1$ to obtain an equation for the optimal neutron batch size.

$$m_{opt} = \sqrt{\frac{h}{\varepsilon_0}\left(1 - \frac{k_1}{k_0}\right)} \tag{44}$$

given the total number of simulated neutron histories, dominance ratio of the system, and relative error in the initial fission source. This equation enables one to determine a value for the neutron batch size that balances its effects on the speed of source convergence and biasing of results.

In order to apply Eq. (44), the dominance ratio and the error in the initial fission source are needed. Fortunately, both quantities can be estimated with reasonable accuracy and effort during an initial stage of the Monte Carlo criticality calculation. We suggest to evaluate these parameters during the simulation of a small fraction (e.g. 1%) of the specified total number of neutron histories.

The dominance ratio can be evaluated by a number of methods, such as the NPM method (Sutton et al., 2011) or the CMFD based method (Herman et al., 2013). The error in the initial fission source can be estimated by the eigenvector of the fission matrix as (Tuttelberg and Dufek, 2014)

$$\tilde{\varepsilon}_0 = \frac{\|\mathbf{s}^{(0)} - \mathbf{q}\|_1}{2m_0} \tag{45}$$

where $\mathbf{s}^{(0)}$ is the initial fission source, m_0 is the neutron batch size chosen for the first n_0 cycles, and $\mathbf{q}$ is the eigenvector calculated from the fission matrix that was sampled during the initial cycles (normalised to the batch size m_0). If the fission matrix is not available, a very rough approximation can, instead, be taken as

$$\tilde{\varepsilon}_0 \cong \frac{\|\mathbf{s}^{(0)} - \mathbf{s}_c/n_0\|_1}{2m_0} \tag{46}$$

where $\mathbf{s}_c$ is the cumulative fission source combined over n_0 cycles. The factor 2 in Eqs. (45) and (46) scales the maximum possible value of $\tilde{\varepsilon}_0$ to one.

The estimation of dominance ratio is improved by simulating more cycles (Nease et al., 2008); and since the bias is of no concern in these initial cycles, we recommend to set a small value for m_0, for example so that $n_0 = m_0^2$. This results in $m_0 = \sqrt[3]{h_0}$, where h_0 is the number of histories used in the estimation stage.

After the initial stage, the estimated values of $\tilde{\varepsilon}_0$ and the dominance ratio are used in Eq. (44) to evaluate the optimal neutron batch size that is then used in the following cycles.

5. Numerical test calculations

5.1. Numerical test model

Numerical test calculations were performed on a model of a common PWR fuel pin cell with parameters specified in Tab. 1. Reflective boundary conditions were applied on radial faces and void boundary conditions on axial faces. This model shares some features of a large core, e.g. a large dominance ratio.

Table 1: Specifications of the pin cell model.

Fuel	UO_2
Cladding material	Zr
Moderator	light water
Radius of fuel pellets	0.41 cm
Outer radius of cladding	0.475 cm
Rod pitch	1.26 cm
Length of the fuel rod	400 cm
^{235}U enrichment	3.1 wt%
Fuel density	10 g/cm^3
Moderator (water) density	0.7 g/cm^3

All numerical calculations were performed by an in-house non-analogue continuous-energy 3D Monte Carlo criticality code using the JEFF3.1 point-wise neutron cross-section library.

5.2. Reference calculation

The correct fission source distribution for the test system is not known exactly; hence, we estimate it by a reference calculation specified in Tab. 2. As the test model is symmetrical, we have additionally symmetrised the source distribution $\mathbf{s}_r$ combined over the active cycles. The dominance ratio was estimated at 0.989 during the reference calculation by the NPM method (Sutton et al., 2011) with a 10 cell axial mesh.

Table 2: Specifications of the reference calculation.

Number of histories per cycle	50,000
Number of active cycles	1,000,000
Number of inactive cycles	10,000
Initial fission source	flat

The reference solution is used in evaluating the error in the cumulative fission source in the test calculations. The scalar error in the cumulative fission source is computed as

$$\varepsilon_c = \frac{\|\mathbf{s}_c/h - \mathbf{s}_r/h_r\|_1}{2} \tag{47}$$

where $\mathbf{s}_c$ and $\mathbf{s}_r$ are the fission sources combined over the cycles of test and reference calculations, respectively, and h_r is the total number of neutron histories simulated in the reference calculation. The factor in the denominator of Eq. (47) ensures the maximal possible value of ε_c to be one.

Note that while the simplified model of the scalar error in the cumulative fission source captures the dependence of the error on the neutron batch size and other parameters, its direct comparison to the error computed by Eq. (47) is not trivial. This is not a problem for the presented optimisation methodology; it is merely an inconvenience when comparing the simplified model to results from test calculations, as the values do not necessarily have to match.

5.3. Demonstration of the simplified error model

The purpose of the calculations presented in this section is to demonstrate the usability of the simplified model of the scalar error in the cumulative fission source, given by Eq. (39). In this test, the simplified model is supplied with the dominance ratio estimated by the reference calculation; the constants B and R are assumed equal to one.

Four calculations, A–D, specified in Tab. 3, were repeated 40 times with various seeds for the random number generator. All calculations were started with a point source placed at one end of the pin, ensuring a large error in the initial fission source. Thus, the model assumes the maximum value $\varepsilon_0 = 1$.

Table 3: Specifications of calculations A–D.

Test calculation	A	B	C	D
Neutron histories per cycle	50	500	5000	50,000
Total number of histories	100 million			

In Fig. 1, the scalar errors in calculations A–D, computed by Eq. (47), are compared to the simplified model, given by Eq. (39). The results demonstrate that the simplified model correctly captures the dependence of the error on the neutron batch size and the total number of simulated neutron histories.

Fig. 1 also shows that performance of the calculation (given here by the error in the cumulative fission source) depends strongly on the neutron batch size; for a specific allocated computing cost (in terms of the total number of simulated neutron histories) the calculation performs best with a specific neutron batch size. For instance, when 10^7 neutron histories are to be simulated, the results achieved by simulating 500 neutron histories per cycle are significantly better than with other chosen values.

5.4. Performance of calculations with optimal neutron batch size

In this section, we demonstrate the performance of Monte Carlo criticality calculations with the optimal neutron batch size estimated by Eq. (44). We wish to separate the effects of simplifications made in deriving Eq. (44) from the effects of errors present in the estimated parameters in Eq. (44); therefore, we use the dominance ratio computed by the reference calculation. Such an accurate estimate of the dominance ratio would not be available in standard calculations; therefore, Sec. 5.5 includes numerical tests

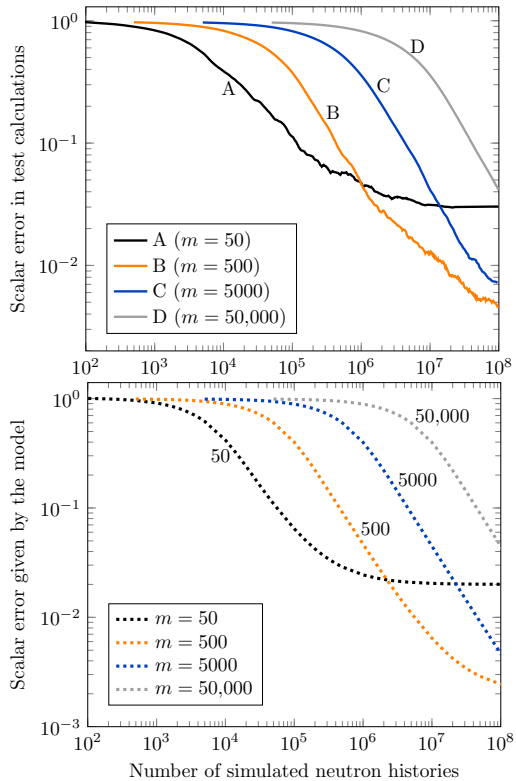

Figure 1: Top: scalar errors in calculations A–D computed by Eq. (47). Bottom: Scalar errors predicted by the simplified model, as in Eq. (39) for $m = 50$, 500, 5000 and 50,000.

where the dominance ratio is computed in the beginning of the calculation, using a relatively small number of neutron histories, as suggested in Sec. 4.

Tab. 4 shows the optimal neutron batch size calculated by Eq. (44) for three values of allocated computing cost (10^8, 10^7 and 10^6 simulated neutron histories); the three cases are marked as E, F, and G. For this, the dominance ratio was set to 0.989, and the relative error in the initial fission source was set to the maximum value $\varepsilon_0 = 1$ (the same initial source was used as in Sec. 5.3).

Table 4: Specifications of calculations E–G.

Test calculation	E	F	G
Total number of histories	10^8	10^7	10^6
Optimal neutron batch size	1050	333	105

Monte Carlo criticality calculations for cases E, F, and G were repeated 40 times with different seeds, and the resulting errors were averaged. Fig. 2 compares the performance of these cases, and demonstrates the effectiveness

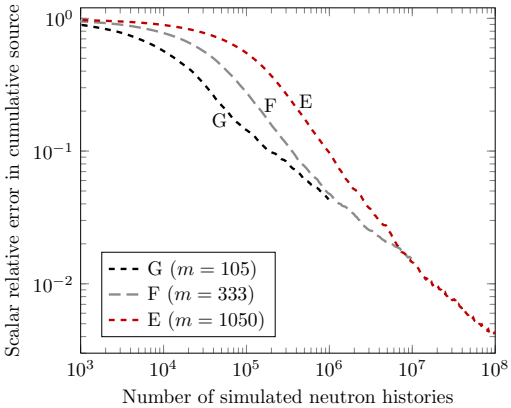

Figure 2: Results of calculations E–G.

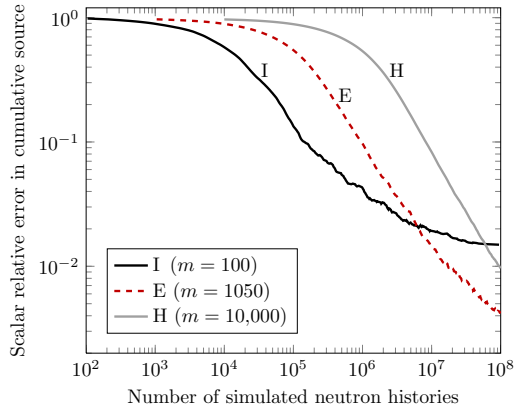

Figure 3: Results of calculations E, H, and I.

of the optimal neutron batch size computed by Eq. (44) for various cases. For instance, when 10^6 neutron histories were simulated, the calculation with the neutron batch size optimised for 10^6 neutron histories (case G) performed better than the calculation with the neutron batch size optimised for 10^8 neutron histories (case E). Nevertheless, we can see that case F (optimised for 10^7 neutron histories) performed similarly to case G when 10^6 neutron histories were simulated, which suggests that the optimal value of the neutron batch size does not necessarily have to be computed very accurately in order to achieve good performance. This simplifies the application of our methodology since the input parameters, such as the dominance ratio or the error in the initial fission source, may be estimated less accurately in the beginning of the calculation.

In this section, we also compare case E (with the neutron batch size optimised for 10^8 histories) to two additional calculations where the neutron batch size was set to suboptimal values of 10,000 (case H) and 100 (case I). Calculations H and I were also repeated 40 times and averaged. Fig. 3 shows that calculation E (optimal) achieved orders of magnitude smaller errors than calculations H and I after simulating 10^8 neutron histories (for which case E was optimised).

5.5. Practical application of the optimisation methodology

The purpose of this section is to test the neutron batch size optimisation methodology for Monte Carlo criticality calculations, as suggested in Sec. 4, assuming no knowledge of the correct dominance ratio or the error in the initial fission source. Therefore, as suggested in Sec. 4, the calculation is split into two stages; the dominance ratio and the error in the initial fission source are estimated in the short first stage, while the neutron batch size is corrected to the optimal value for the second stage.

The total allocated computational cost was set to 10^8 neutron histories for this test. As suggested in Sec. 4, we allocated 1% of the computing cost (10^6 neutron histories) to the first stage of the calculation. According to suggestions in Sec. 4, the neutron batch size for the first stage was set to $\sqrt[3]{10^6} = 100$.

During the first stage, the dominance ratio was estimated at 0.9876 by the NPM method; in order to keep the method general and not optimised for a specific test model, a $3 \times 3 \times 3$ spatial mesh was used. The error in the initial fission source was estimated at 0.9941. Based on these values, the optimal neutron batch size was evaluated at 1120, and the batch size was changed to this value for the second stage of the calculation. The value of the dominance ratio estimated during the first step of this calculation does not differ much from the value computed during the reference calculation; hence, the optimal value of the neutron batch size calculated here (1120) does not differ much from the test case E (1050).

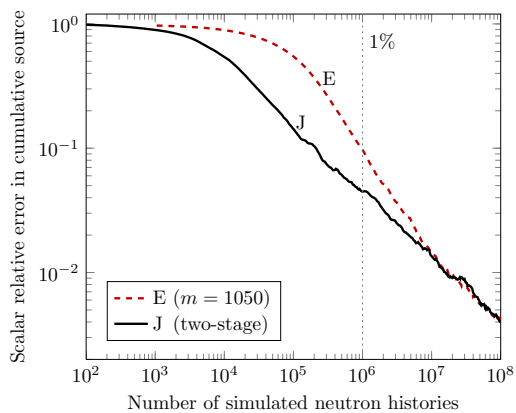

Figure 4: Results of calculations J (two-stage) and E.

The two-stage calculation was repeated 40 times, and results were averaged, as in all previous calculations. Fig. 4 compares the performance of this two-stage calculation (marked as case J) to the test case E (that used the neutron batch size optimised for 10^8 neutron histories). As can be seen, both calculations perform equally well when 10^8 neutron histories are simulated. Naturally, the two-stage calculation converged faster during the first stage, as the neutron batch size was forced to be small; however, this did not change the final results.

6. Conclusions

The results of numerical test calculations showed that the simplified model of the scalar error in the cumulative fission source captures well both the convergence rate and the presence of source bias. Also, the neutron batch size optimisation methodology, that was derived from the simplified error model, performed well in practical applications, ensuring maximal efficiency. The optimisation method is general in nature and implementable in any power method based Monte Carlo code that comes equipped with a dominance ratio estimation procedure.

It should be noted that the optimal neutron batch size may also be affected by the use of parallelised calculations; for instance, the master-slave parallel-computing scheme performs better with a larger neutron batch size. Nevertheless, the optimisation methodology derived in this paper does not consider the efficiency of various parallel-computing schemes on different computer architectures. This problem may be considered in future work.

Acknowledgements

We would like to thank Vasily Arzhanov (KTH) for helpful discussions and comments.

This research was supported by Estonian scholarship program Kristjan Jaak, which is funded and managed by Archimedes Foundation in collaboration with the Ministry of Education and Research.

This work was partly funded by the European Commission under the High Performance Monte Carlo Reactor Core Analysis (HPMC) project, within the 7th EU Framework Program, Project Number 295971.

References

Brissenden, R. J., Garlick, A. R., 1986. Biases in the estimation of k_{eff} and its error by Monte Carlo methods. Annals of Nuclear Energy 13 (2), 63–83.

Brown, F. B., 2009. A review of best practices for Monte Carlo criticality calculations. Tech. Rep. LA-UR-09-03136, Los Alamos National Laboratory.

Brown, F. B., Carney, S. E., Kiedrowski, B. C., Martin, W. R., 2013. Fission matrix capability for MCNP, part I – theory. Tech. Rep. LA-UR-13-20429, Los Alamos National Laboratory.

Carter, L. L., McCormick, N. J., 1969. Source convergence in Monte Carlo calculations. Nuclear Science and Engineering 36, 438–441.

Dubi, A., Elperin, T., 1985. On the markov chain analysis of source iteration Monte Carlo procedures for criticality problems: II. Nuclear Science and Engineering 91 (1), 77–83.

Enosh, M., Shalitin, D., Yeivin, Y., 1990. The bias in Monte Carlo eigenvalue calculations. Progress in Nuclear Energy 24, 259–269.

Gast, R. C., 1969. Monte Carlo eigenfunction iteration strategies that are and are not fair games. Tech. Rep. WAPD-TM-878.

Gast, R. C., Candelore, N. R., 1974. Monte Carlo eigenfunction strategies and uncertainties. In: Proceedings of NEACRP Meeting of a Monte Carlo Study Group. Argonne National Laboratory.

Gelbard, E. M., 1992. Biases in Monte Carlo eigenvalue calculations. In: IMACS-International Symposium on Scientific Computing and Mathematical Modeling. Bangalore, India.

Gelbard, E. M., Gu, A. G., 1994. Biases in Monte Carlo eigenvalue calculations. Nuclear Science and Engineering 117, 1–9.

Gelbard, E. M., Prael, R. E., July 1974. Monte Carlo work at Argonne National Laboratory. In: Proceedings of NEACEP Monte Carlo Specialists Meeting. Argonne National Laboratory.

Goult, R. J., Hoskins, R. F., Milner, J. A., Pratt, M. J., 1975. Computational Methods in Linear Algebra. Wiley.

Herman, B. R., Forget, B., Smith, K., November 2013. Utilizing CMFD in OpenMC to estimate dominance ratio and adjoint. In: Transactions of the American Nuclear Society. Vol. 109. Washington, D.C.

Nease, B. R., 2008. Time series analysis of Monte Carlo neutron transport calculations. Ph.D. thesis, University of New Mexico.

Nease, B. R., Brown, F. B., Ueki, T., Sept 2008. Dominance ratio calculations with MCNP. In: Proc. Int. Topical Mtg. on Physics of Reactors.

Nease, B. R., Ueki, T., 2009. Time series analysis and Monte Carlo methods for eigenvalue separation in neutron multiplication problems. Journal of Computational Physics 228, 8525–8547.

Sutton, T. M., Romano, P. K., Nease, B. R., 2011. On-the-fly Monte Carlo Dominance Ratio calculation using the Noise Propagation Matrix. Progress in Nuclear Science and Technology 2, 749–756.

Tuttelberg, K., Dufek, J., 2014. Estimation of errors in the cumulative Monte Carlo fission source. Annals of Nuclear Energy. Accepted for publication.

Ueki, T., Brown, F. B., Parsons, D. K., Kornreich, D. E., 2003. Autocorrelation and dominance ratio in Monte Carlo criticality calculations. Nuclear Science and Engineering 145, 279–290.

Ueki, T., Brown, F. B., Parsons, D. K., Warsa, J. S., 2004. Time series analysis of Monte Carlo fission sources—I: Dominance Ratio computation. Nuclear Science and Engineering 148, 374–390.

Zolotukhin, V. G., Maiorov, L. V., 1983. An estimate of the systematic errors in the calculations of criticality by the Monte Carlo method. Atomnaya Energia 55 (3), 173.